determining the abilities of oligopeptides as a CPP, we selected various octapeptides that consist of one kind of amino acid (octa-tyrosine (Y8: hydrophobic), octa-asparagine (N8: hydrophilic), octa-glutamic acid (E8: hydrophilic and anionic), octa-histidine (H8: hydrophilic and weakly cationic), octa-lysine (K8: hydrophilic and cationic), or octa-arginine (R8: hydrophobic and cationic)). These peptides were conjugated with PMBN/PLA/QD respectively. A HeLa cell (seeded into 12-well plates at 1.0×10^4 cell/well in 1 mL of culture medium) was incubated with each octapeptide-conjugated PMBN/PLA/QD for 5 h. The quantification of the uptake of PMBN/PLA/QD was performed. As shown in Fig. 11, only K8 and R8 conjugated PMBN/PLA/QD could internalize in HeLa cells. This result indicated that the hydrophilic and cationic nature of oligopeptides play a key role in the cell membrane permeation. In order to understand the mechanism of cell penetration induced by these hydrophilic and cationic oligopeptides, it will be required to investigate the relationship between surface cationic density on the nanoparticles and cell membrane permeation.

5. Conclusion

Many important applications of nanotechnology would not be achievable without proper design of nanosturcture. As integrative field of biomedical nanotechnology evolves, more systematic approaches for the chemical design of nanostructures will be required. Furthermore, as the researchers start to construct multifunctional nanostructures, the interface between nanostructure and biological environments will be critical. In this study, our artificial cell membrane–biointerface can provide the imaging probes with the abilities to suppress completely the interactions between imaging probes themselves and cells. This biointerface is necessary to study the fundamental information of the biomolecular behavior in cellular environments. We described the kinetic behavior in cytoplasm of our polymer nanoparticles containing QDs with artificial cell membrane–biointerface. Although these nanoparticles can avoid the nonselective cellular uptake from mammalian cells, when bioactive molecules were immobilized, our nanoparticles can provide the various information about the specific interaction between biomolecules and cells. From these findings, we conclude that the nanoparticles are candidates for the role of stable and highly sensitive fluorescent bioimaging probes in the fields of nanotechnology. Controlling interactions with cells is receiving considerable importance in biomedical fields, including nanobioengineering and cell and tissue engineering. The bioinspired interfaces described here are a promising design for revealing a universal platform that integrates polymer chemistry; material science; and engineering, biochemistry, cell biology, and nanofabrication.

Acknowledgements

This research was partially supported by Special Coordination Funds for Promoting Science and Technology from the Ministry of Education, Culture, Sports, Science, and Technology, Japan.

References

[1] S.J. Singer, G.L. Nicholson, The fluid mosaic model of the structure of cell membranes, Science 175 (1972) 720–731.
[2] P.L. Yeagle, The Membranes of Cells, second ed.Academic Press, New York, 1993.
[3] J.A. Hayward, D. Chapman, Biomembrane surfaces as models for polymer design: the potential for haemocompatibility, Biomaterials 5 (1984) 135–142.
[4] J.J. Ramsden, G.I. Bachmanova, A.I. Archakov, Immobilization of proteins to lipid bilayers, Biosens. Bioelectron. 5 (1996) 523–528.
[5] X.L. Sun, W. Cui, T. Kai, E.L. Chaikof, A facile synthesis of bifunctional phospholipids for biomimetic membrane engineering, Tetrahedron 60 (2004) 11765–11770.
[6] L. Brunsveld, H. Waldmann, D. Huster, Membrane binding of lipidated Ras peptides and proteins—the structural point of view, Biochim. Biophys. Acta 1788 (2009) 273–288.
[7] H.M. Cho, D.Y. Cho, J.Y. Jeon, S.Y. Hwang, I.S. Ahn, J. Choo, E.K. Lee, Fabrication of protein-anchoring surface by modification of SiO_2 with liposomal bilayer, Colloids Surf. B: Biointerfaces 75 (2010) 209–213.
[8] K. Ishihara, J. Watanabe, Y. Iwasaki, Bioinspired polymer surfaces for prevention of bioresponse, Mater. Sci. Forum 426–432 (2003) 3171–3176.
[9] J. Watanabe, J.-W. Park, T. Ito, M. Takai, K. Ishihara, Biofunctionalization of phospholipid polymer nanoparticles, in: C.S.S.R. Kumar (Ed.), Nanotechnologies for the Life Science, Biofunctionalizaation of Nanomaterials, vol. 1, Wiley-VCH, Weinheim, 2005, pp. 125–149.
[10] J. Watanabe, K. Ishihara, Biointerface, bioconjugation, and biomatrix based on bioinspired phospholipid polymers, in: H.S. Nalwa (Ed.), Handbook of Nanostructured Biomaterials and Their Applications in Nanobiotechnology vol. 1, American Scientific Publishers, 2005, pp. 129–165.
[11] J. Watanabe, K. Ishihara, Establishing ultimate biointerfaces covered with phosphorylcholine groups, Colloids Surf. B: Biointerfaces 65 (2008) 155–165.
[12] K. Ishihara, K. Nishizawa, Y. Goto, M. Takai, Bioinspired polymer surfaces for nanodevices and nanomedicine, Adv. Sci. Technol. 57 (2008) 5–14.
[13] K. Ishihara, T. Ueda, N. Nakabayashi, Preparation of phospholipid polymers and their properties as polymer hydrogel membrane, Polym. J. 22 (1990) 355–360.
[14] T. Ueda, H. Oshida, K. Kurita, K. Ishihara, N. Nakabayashi, Preparation of 2-methacryloyloxyethyl phosphorylcholine copolymers with alkyl methacrylates and their blood compatibility, Polym. J. 24 (1992) 1259–1269.
[15] K. Ishihara, R. Aragaki, T. Ueda, A. Watanabe, N. Nakabayashi, Reduced thrombogenicity of polymers having phospholipid polar groups, J. Biomed. Mater. Res. 24 (1990) 1069–1077.
[16] K. Ishihara, N.P. Ziats, B.P. Tierney, N. Nakabayashi, J.M. Anderson, Protein adsorption from human plasma is reduced on phospholipid polymers, J. Biomed. Mater. Res. 25 (1991) 1397–1407.
[17] K. Ishihara, H. Oshida, Y. Endo, T. Ueda, A. Watanabe, N. Nakabayashi, Hemocompatibility of human whole blood on polymers with a phospholipid polar group and its mechanism, J. Biomed. Mater. Res. 26 (1992) 1543–1552.
[18] T.A. Snyder, H. Tsukui, S. Kihara, T. Akimoto, K.N. Litwak, M.V. Kameneva, Preclinical biocompatibility assessment of the EVAHEART ventricular assist device: coating comparison and platelet activation, J. Biomed. Mater. Res. A 81 (2007) 85–92.
[19] G.J. Myers, D.R. Johnstone, W.J. Swyer, S. McTeer, S.L. Maxwell, C. Squires, S.N. Ditmore, C.V. Power, L.B. Mitchell, J.E. Ditmore, L.D. Aniuk, G.M. Hirsch, K.J. Buth, Evaluation of mimesys phosphorylcholine (PC)-coated oxygenators during cardiopulmonary bypass in adults, J. Extra-Corpor. Technol. 35 (2003) 6–12.
[20] M. Kyomoto, T. Moro, T. Konno, H. Takadama, N. Yamawaki, H. Kawaguchi, Y. Takatori, K. Nakamura, K. Ishihara, Enhanced wear resistance of modified cross-linked polyethylene by grafting with poly(2-methacryloyloxyethyl phosphorylcholine), J. Biomed. Mater. Res. A 82A (2007) 10–17.
[21] A.L. Lewis, L.A. Tolhurst, P.W. Stratford, Analysis of a phosphorylchline-based polymer coating on a coronary stent pre- and post-implantation, Biomaterials 23 (2002) 1697–1706.
[22] K. Ishihara, M. Takai, Bioinspired interfaces for nanobiodevices based on phospholipid polymer chemistry, J. R. Soc. Interface 6 (2009) S279–S291.
[23] K. Nishizawa, T. Konno, M. Takai, K. Ishihara, Bioconjugated phospholipid polymer biointerface for ELISA, Biomacromolecules 9 (2008) 403–407.
[24] E. Kharlampieva, D. Pristinski, S.A. Sukhishvili, Hydrogen-bonded multilayers of poly(carboxybetaine)s, Macromolecules 40 (2007) 6967–6972.
[25] Y. Chang, S.-C. Liao, A. Higuchi, R.-C. Ruaan, C.-W. Chu, W.-Y. Chen, A highly stable nonbiofouling surface with well-packed grafted zwitterionic polysulfobetaine for plasma protein repulsion, Langmuir 24 (2008) 5453–5458.
[26] Y.-C. Chianga, Y. Changb, A. Higuchia, W.-Y. Chena, R.-C. Ruaana, Sulfobetaine-grafted poly(vinylidene fluoride) ultrafiltration membranes exhibit excellent antifouling property, J. Membr. Sci. 339 (2009) 151–159.
[27] H. Vaisocherová, W. Yang, Z. Zhang, Z. Cao, G. Cheng, M. Piliarik, J. Homola, S. Jiang, Ultralow fouling and functionalizable surface chemistry based on a zwitterionic polymer enabling sensitive and specific protein detection in undiluted blood plasma, Anal. Chem. 80 (2008) 7894–7901.
[28] G. Cheng, G. Li, H. Xue, S. Chen, J.D. Bryers, S. Jiang, Zwitterionic carboxybetaine polymer surfaces and their resistance to long-term biofilm formation, Biomaterials 30 (2009) 5234–5240.
[29] S. Tugulu, H.-A. KlokStability, Nonfouling properties of poly(poly(ethylene glycol) methacrylate) brushes under cell culture conditions, Biomacromolecules 9 (2008) 906–912.
[30] X.-D. Huang, K. Yao, H. Zhang, X.-J. Huang, Z.-K. Xu, Surface modification of silicone intraocular lens by 2-methacryloyloxyethyl phosphoryl-choline binding to reduce *Staphylococcus epidermidis* adherence, Clin. Exp. Ophthalmol. 35 (2007) 462–467.
[31] W. Feng, S. Zhu, K. Ishihara, J.L. Brash, Adsorption of fibrinogen and lysozyme on silicon grafted with, poly(2-methacryloyloxyethyl phosphorylcholine) via surface-initiated atom transfer, radical polymerization, Langmuir 21 (2005) 5980–5987.
[32] S.F. Rose, S. Okere, G.W. Hanlon, A.W. Lloyd, A.L. Lewis, Bacterial adhesion to phosphorylcholine-based polymers with varying cationic charge and the effect of heparin pre-adsorption, J. Mater. Sci. Mater. Med. 16 (2005) 1003–1015.
[33] J.-J. Yuan, A. Schmid, S.P. Armes, Facile synthesis of highly biocompatible poly(2-(methacryloyloxy)ethyl phosphorylcholine)-coated gold nanoparticles in aqueous solution, Langmuir 22 (2006) 11022–11027.
[34] T. Ueda, K. Ishihara, N. Nakabayashi, Adsorption–desorption of proteins on phospholipid polymer surfaces evaluated by dynamic contact angle measurement, J. Biomed. Mater Res. 29 (1995) 381–387.
[35] A. Yamasaki, Y. Imamura, K. Kurita, Y. Iwasaki, N. Nakabayashi, K. Ishihara, Surface mobility of polymers having phosphorylcholine groups connected with various

bridging units and their protein adsorption-resistant properties, Colloids Surf. B: Biointerfaces 28 (2003) 53–62.
[36] K. Ishihara, H. Nomura, T. Mihara, K. Kurita, Y. Iwasaki, N. Nakabayashi, Why do phospholipid polymer reduce protein adsorption? J. Biomed. Mater. Res. 39 (1998) 323–330.
[37] T. Morisaku, J. Watanabe, T. Konno, M. Takai, K. Ishihara, Hydration of phosphorylcholine groups attached to highly swollen polymer hydrogels studied by thermal analysis, Polymer 49 (2008) 4652–4657.
[38] H. Kitano, M. Imai, T. Mori, M. Gemmei-Ide, Y. Yokoyama, K. Ishihara, Structure of water in the vicinity of phospholipid analog copolymers as studied by vibrational spectroscopy, Langmuir 19 (2003) 10260–10266.
[39] D.R. Lu, S.J. Lee, K. Park, Calculation of solvetion interaction energies for protein adsorption on polymer surface, J. Biomater. Sci. Polym. Edn. 3 (1991) 127–147.
[40] K. Takei, K. Konno, J. Watanabe, K. Ishihara, Regulation of enzyme–substrate complexation by phospholipid polymer conjugates for cell engineering, Biomacromolecules 5 (2004) 858–862.
[41] K. Kinoshita, K. Fujimoto, T. Yakabe, S. Saito, Y. Hamaguchi, T. Kikuchi, K. Nonaka, S. Murata, D. Masuda, W. Takada, S. Funaoka, S. Arai, H. Nakanishi, K. Yokoyama, K. Fujiwara, K. Matsubara, Multiple primer extension by DNA polymerase on a novel plastic DNA array coated with a biocompatible polymer, Nucleic Acids Res. 35 (e3) (2007) 1–9.
[42] J. Watanabe, K. Ishihara, Multiple protein immobilized phospholipid polymer nanoparticles: effect of spacer length on residual enzymatic activity and molecular diagnosis, Nanobiotechnology 3 (2008) 76–82.
[43] K. Nishizawa, M. Takai, K. Ishihara, Stabilization of phospholipid polymer surface with three-dimensional; nanometer-scales structure for highly sensitive immunoassay, Colloids Surf. B: Biointerfaces 77 (2010) 263–269.
[44] K. Ishihara, Y. Iwasaki, N. Nakabayashi, Polymeric lipid nanosphere constituted of poly(2-methacryloyloxyethyl phosphorylcholine-co-*n*-butyl methacrylate), Polym. J. 31 (1999) 1231–1236.
[45] K. Konno, J. Watanabe, K. Ishihara, Conjugation of enzymes on polymer nanoparticles covered with phosphorylcholine groups, Biomacromolecules 5 (2004) 342–347.
[46] J. Watanabe, K. Ishihara, Single step diagnosis system using the FRET phenomenon induced by antibody-immobilized phosphorylcholine group-covered polymer nanoparticles, Sens. Actuat. B: Chem. 129 (2008) 87–93.
[47] J. Watanabe, K. Ishihara, Sequential enzymatic reactions and stability of biomolecules immobilized onto phospholipid polymer nanoparticles, Biomacromolecules 7 (2006) 171–175.
[48] T. Ito, J. Watanabe, M. Takai, T. Konno, Y. Iwasaki, K. Ishihara, Dual mode bioreactions on polymer nanoparticles covered with phosphorylcholine group, Colloids Surf. B: Biointerfaces 50 (2006) 55–60.
[49] Y. Goto, R. Matsuno, T. Konno, M. Takai, K. Ishihara, Polymer nanoparticles covered with phosphorylcholine groups and immobilized with antibody for high-affinity separation of proteins, Biomacromolecules 9 (2008) 828–833.
[50] A.A. Garcia, Bioseparation Process Science, Blackwell Science Inc., Cambridge, MA, 1999.
[51] A.M. Smith, H. Duan, A.M. Mohs, S. Ni, Bioconjugated quantum dots for in vivo molecular and cellular imaging, Adv. Drug Deliv. Rev. 60 (2008) 1226–1240.
[52] T. Jamiesona, R. Bakhshia, D. Petrovaa, R. Pococka, M. Imanib, A.M. Seifaliana, Biological applications of quantum dots, Biomaterials 28 (2007) 4717–4732.
[53] A.F.E. Hezinger, J. Teßmar, A. Gopferich, Polymer coating of quantum dots—a powerful tool toward diagnostics and sensorics, Eur. J. Pharm. Biopharm. 68 (2008) 138–152.
[54] Y. Goto, R. Matsuno, T. Konno, M. Takai, K. Ishihara, Artificial cell membrane-covered nanoparticles embedding quantum dots as stable and highly sensitive fluorescence bioimaging probes, Biomacromolecules 9 (2008) 3252–3257.
[55] X. Wu, H. Liu, J. Liu, K.N. Haley, J.A. Treadway, J.P. Larson, N. Ge, F. Peale, M.P. Bruchez, Immunofluorescent labeling of cancer marker Her2 and other cellular targets with semiconductor quantum dots, Nat. Biotechnol. 21 (2003) 41–46.
[56] B. Dubertret, P. Skourides, D.J. Norris, V. Noireaux, A.H. Brivanlou, A. Libchanber, In vivo imaging of quantum dots encapsulated in phospholipid micelles, Science 298 (2002) 1759–1762.
[57] T. Moro, Y. Takatori, K. Ishihara, T. Konno, Y. Takigawa, T. Matsushita, U.I. Chung, K. Nakamura, H. Kawaguchi, Surface grafting of artificial joints with a biocompatible polymer for preventing periprosthetic osteolysis, Nat. Mater. 3 (2004) 829–836.
[58] I.A. Khalil, K. Kogure, S. Futaki, S. Hama, H. Akita, M. Ueno, H. Kishida, M. Kudoh, Y. Mishima, K. Kataoka, M. Yamada, H. Harashima, Octaarginine-modified multifunctional envelope-type nanoparticles for gene delivery, Gene Ther. 14 (2007) 682–689.
[59] A. El-Sayed, I.A. Khalil, K. Kogure, S. Futaki, H. Harashima, Octaarginine- and octalysine-modified nanoparticles have different modes of endosomal escape, J. Biol. Chem. 283 (2008) 23450–23610.

Reactive & Functional Polymers 71 (2011) 350–355

Contents lists available at ScienceDirect

Reactive & Functional Polymers

journal homepage: www.elsevier.com/locate/react

Adhesion force of proteins against hydrophilic polymer brush surfaces

Yuuki Inoue [a], Tomoaki Nakanishi [a], Kazuhiko Ishihara [a,b,c,*]

[a] Department of Materials Engineering, School of Engineering, The University of Tokyo, 7-3-1, Hongo, Bunkyo-ku, Tokyo 113-8656, Japan
[b] Department of Bioengineering, School of Engineering, The University of Tokyo, 7-3-1, Hongo, Bunkyo-ku, Tokyo 113-8656, Japan
[c] Core Research for Evolutional Science and Technology (CREST), Japan Science and Technology Agency (JST), 5 Sanban-cho, Chiyoda-ku, Tokyo 102-0075, Japan

ARTICLE INFO

Article history:
Available online 19 November 2010

Keywords:
Polymer brush layer
Surface-initiated atom transfer radical polymerization
Surface modification
Atomic force microscopy
Adhesion force of proteins

ABSTRACT

Protein adsorption occurs on the surface of biomaterials when they are exposed to physiological environments. The protein adsorption layer induces severe biological responses, including cellular reactions. Protein adsorption layers are formed mainly by two distinct processes: monolayer adsorption of proteins on the surface and a subsequent additional adsorption on the first layer to form a multilayer. Therefore, evaluating the first protein adsorption is important to understand the biological responses on the surface of materials. In this study, we applied the atomic force microscopic (AFM) technique to directly measure the adhesion force of proteins against the surface (i.e., the interaction between proteins and surface). We also prepared hydrophilic polymer brush surfaces with well-known high repellency against protein adsorption through surface-initiated atom transfer radical polymerization. Polymer brush layers have a well-defined surface structure; therefore, it could be a good model for clarifying the relationship between the surface structure and protein adsorption behavior. The influence of chemical structure of monomer unit and thickness of polymer brush layers on the adhesion force of proteins was discussed here, while that of graft density was not discussed. The adhesion force of bovine serum albumin (BSA) immobilized on an AFM cantilever against the thin polymer brush surfaces differed from the chemical structures of the monomer unit. The adhesion force of BSA decreased with increasing thickness of the polymer brush layer, and there was little difference in the adhesion force of BSA against the thick polymer brush surfaces regardless of the chemical structure of the monomer unit. The results demonstrate that the thickness of the polymer brush layer would be an important parameter that reduced the interaction between proteins and surfaces compared with the chemical structure of the monomer unit.

1. Introduction

Protein adsorption on the surface of materials is an important factor that determines subsequent biological responses, including cellular reactions. In particular, nonspecific protein adsorption and deposition on the surface may result in several serious problems, such as immunoreaction, blood coagulation, and inflammatory reaction [1]. A variety of polymeric biomaterial surface designs have been proposed to suppress nonspecific protein adsorption, such as induction of higher polymer chain mobility by poly(ethylene oxide) [2–4] and construction of artificial cell membrane structures by using phospholipid polymers [5–8]. In recent years, surface-initiated grafting of functional monomers to obtain a polymer brush structure has attracted much attention in biomedical research because it restricts protein adsorption to 5 ng/cm^2, which is approximately 300 times less than the protein adsorption mass on conventional materials, including polystyrene for cell culture, glass, etc. [9–18]. On the other hand, the mechanism for obtaining high repellency against protein adsorption in the polymer brush structure is still unclear.

Protein adsorption on the surface in physiological environments involves two stages. First, proteins directly adsorb on the surface of the materials through several kinds of intermolecular interactions between proteins and the surface, occurring under aqueous conditions, which form a single layer of adsorbed proteins. Second, proteins interact with the preadsorbed protein monolayer, the conformation of which would be changed by the interaction with the surface of materials. In this regard, it is important to characterize the direct interactions between proteins and the surface. Measurement of direct interaction is distinctly different from quantification of the protein adsorption mass on the surface of a material; the latter merely estimates the amount of whole proteins adsorbed on the multilayer. Atomic force microscopy (AFM) allows the quantification of the specific force between the biomolecules immobilized on a given surface and probes, such as antigen–antibody [19] and ligand–receptor [20]. In addition, the direct force of nonspecific interactions between proteins and several kinds of

* Corresponding author at: Department of Materials Engineering, School of Engineering, The University of Tokyo, 7-3-1, Hongo, Bunkyo-ku, Tokyo 113-8656, Japan. Tel.: +81 3 5841 7124; fax: +81 3 5841 8647.
E-mail address: ishihara@mpc.t.u-tokyo.ac.jp (K. Ishihara).

1381-5148/$ - see front matter © 2010 Elsevier Ltd. All rights reserved.
doi:10.1016/j.reactfunctpolym.2010.11.017

self-assembled monolayers [21] and grafted polymer surfaces [22] has also been evaluated. In all previous studies, the forces in the order of a few piconewtons were detected, and the phenomena that occurred in the microenvironment of the biomaterial surface were manifested. To our knowledge, no research has been conducted on the direct measurement of the adhesion force of proteins against the polymer brush layers. Because the polymer brush layers have a well-defined surface structure, analysis of the adhesion force of proteins against them could provide a novel understanding of the behavior of protein adsorption on a biomaterial surface.

In this study, we prepared poly(2-methacryloyloxyethyl phosphorylcholine) (PMPC), poly(oligo(ethylene glycol) monomethacrylate) (POEGMA), and poly(2-hydroxyethyl methacrylate) (PHEMA) brush layers on silicon wafers by using the surface-initiated atom transfer radical polymerization (SI-ATRP) method with a sacrificial initiator. To obtain information on the polymer brush layer, we characterized its surface structure and properties by using AFM, X-ray photoelectron spectroscopy (XPS), spectroscopic ellipsometry, and static contact angle measurement under dry and wet conditions. Then, the adhesion force of proteins against these polymer brush layers was quantified using an AFM with a protein-immobilized cantilever. This study analyzed the effect of layer thickness and monomer moiety of well-characterized polymer brush structures on the adhesion force of proteins. The results demonstrate that the thickness of the polymer brush layer has a relatively larger influence on the reduction of the adhesion force of proteins than the chemical structure of the polymer brush layer.

2. Experimental

2.1. Materials

MPC was synthesized and purified using a previously reported method [5]. OEGMA with a repeating number (n) of ethylene glycols of 4, HEMA, and bovine serum albumin (BSA) were purchased from Sigma–Aldrich Co. (St. Louis, MO, USA). Copper (I) bromide (CuBr), 2,2′-bipyridyl (bpy), and ethyl-2-bromoisobutyrate (EBIB) were purchased from Sigma–Aldrich Co. and were directly used as received. Triethylamine (TEA) was purchased from Kanto Chemical Co. (Tokyo, Japan) and used after distillation at 95 °C. All other reagents and solvents of extra-pure grade were commercially available and were used as purchased. Silicon wafers were purchased from Furuuchi Chemical Co. (Tokyo, Japan); the surface of the silicon wafers was coated with approximately 10-nm-thick SiO_2 layers. High-purity grade oxygen and argon gases were used.

2.2. Preparation of initiator-immobilized substrate

To prepare the homogeneous monolayer of the initiator on the silicon wafers, a surface-immobilizing initiator, 3-(2-bromoisobutyryl)decyl dimethylchlorosilane (BrC10DMCS), was synthesized as previously described [23]. The silicon wafers, which were adequately rinsed by sonication with hexane, ethanol, and acetone, and etched by using oxygen plasma (PR500; Yamato Scientific Co. Ltd., Tokyo, Japan), were immersed in a 50 mmol/L solution of BrC10DMCS in toluene for 72 h under inert conditions in the presence of TEA as a catalyst and acid scavenger. The wafers were removed from the solution, rinsed with toluene and methanol, and dried *in vacuo* until they were used for graft polymerization.

2.3. Preparation of polymer brush layers

MPC, OEGMA, and HEMA were graft polymerized from the BrC10DMCS-immobilized substrate by using SI-ATRP as follows [14]. CuBr, bpy, and each monomer in a particular molar ratio were placed in a glass tube and dehydrated; thereafter, degassed solvents were added into the glass tube. The following solvents were used: methanol for MPC and HEMA at monomer concentrations of 0.56 mol/L and 2.0 mol/L, respectively, and a mixture of methanol and tetrahydrofuran (THF) (1:1 by volume) for OEGMA at a concentration of 0.50 mol/L. Argon was bubbled into each monomer solution at room temperature for 10 min. The BrC10DMCS-immobilized substrate was then immersed in the solution, and EBIB was simultaneously added as the free initiator at a defined concentration. After the glass tubes were sealed, polymerization was performed at room temperature with stirring. After 24 h, the substrate was removed from the polymerization solution, rinsed, and purified with ultrasonication for 5 min in methanol and dried in a nitrogen stream. We prepared polymer brush layers for each type of monomer at [Monomer]/[Initiator] ratios of 10, 20, and 50; the ratio was represented after the abbreviation of the polymer name (i.e., PMPC10, POEGMA10, and PHEMA10). The chemical structures of the monomer units used for the synthesis of PMPC, POEGMA, and PHEMA brush layers are shown in Fig. 1.

The conversion of monomers in different polymerization solutions was determined using nuclear magnetic resonance spectroscopy (^{1}H NMR; JEOL, Tokyo, Japan). The molecular weights and polydispersities of free polymers in the reaction solutions were determined through gel permeation chromatography (GPC) using a methanol/water mixture (70:30) containing 10 mmol/L lithium bromide as an eluent and poly(ethylene glycol) as standard.

2.4. Surface characterization

The composition of surface elements was determined using an XPS (AXIS-Hsi; Shimadzu/Kratos, Kyoto, Japan) with a magnesium anode nonmonochromatic source. The samples were completely dried *in vacuo* before the measurement. High-resolution scans for C_{1s}, O_{1s}, N_{1s}, and P_{2p} were acquired at a takeoff angle of 90° for the photoelectrons. All binding energies were referred to the C_{1s} peak at 285.0 eV.

The thickness of the grafted polymer layers present on the BrC10DMCS-immobilized substrates was determined under dry conditions by using a spectroscopic ellipsometer (J.A. Woollam

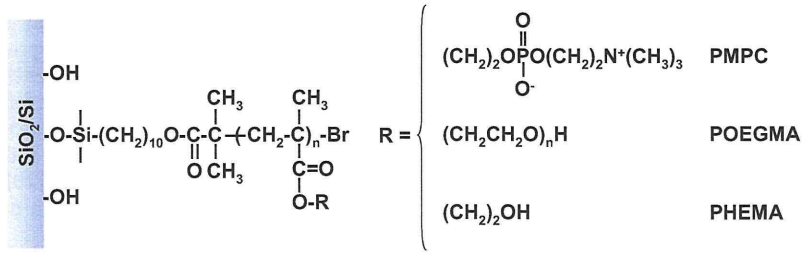

Fig. 1. Chemical structures of the monomer units used for the synthesis of polymer brush layers on the silicon wafers.

Co. Inc., Tokyo, Japan). The BrC10DMCS-immobilized substrate and each polymer brush layer were measured at an incident angle of 70° in the visible region. The thickness of the grafted polymer layers was determined using the Cauchy layer model with an assumed refractive index of 1.49 at 632.8 nm. The graft density (σ [chains/nm^2]) was calculated from the ellipsometric thickness determined for each grafted polymer layer by using the equation:

$$\sigma = h\rho N_A/M_n, \quad (1)$$

where h is the ellipsometric thickness (nm), ρ is the density of each dry polymer (1.30 g/cm^3 for PMPC [13] and 1.15 g/cm^3 for POEGMA and PHEMA [9]), N_A is Avogadro's number, and M_n is the absolute molecular weight of the polymer chains on the surface, which was estimated from the polymerization degree determined using the ^{1}H NMR spectrum of each free polymer. This estimation has been validated for polystyrene and poly(methyl methacrylate (MMA)) [24,25].

The surface morphology of the polymer brush layers under aqueous conditions was observed using an AFM (Nanoscope IIIa; Nihon Veeco, Tokyo, Japan) operated in the tapping mode. The measurements were performed using a standard cantilever at a scan rate of 1.0 Hz, and a scan size of 1 μm × 1 μm. Before the measurements, the samples were immersed in aqueous medium for 24 h. The root mean square (RMS) of the surface roughness was calculated from the roughness profiles.

The static water contact angles under dry conditions and air contact angles in an aqueous medium by captive bubble methods were measured using a goniometer (CA-W; Kyowa Interface Science Co., Tokyo, Japan) at room temperature. The samples were completely dried *in vacuo* before the measurement of static water contact angle. Water droplets of 3 μL volume were brought in contact with the substrates. On the other hand, the samples were immersed in water for 24 h before the measurement of air contact angle. Air bubbles of 5 μL volume were brought in contact with the substrates. All contact angles were directly measured from the photographic images. We show the supplementary angle (180°–θ) of the static air bubble contact angle in aqueous conditions (θ) for easy comparison with static water contact angles in dry conditions. Data were collected for more than three positions for each sample.

2.5. Protein adhesion force measurement

BSA was covalently immobilized on an AFM cantilever through the condensation reaction between the amino groups in the protein and the carboxyl groups on the AFM cantilever [21]. Commercially available 200-μm-long V-shaped Si_3N_4 cantilevers (OTR8; Veeco NanoProbe Tips) with an announced spring constant of 0.15 N/m were used. Gold film was prepared on the Si_3N_4 cantilever by using plasma spattering with 3.0 nm adhesion layer of Cr followed by 27 nm of Au. The oxygen-plasma-treated Au-coated cantilever was immersed in 1.0 mmol/L solution of 11-mercaptoundecanoic acid in ethanol for 1 h to form a carboxyl group-terminated self-assembled monolayer (COOH-SAM). After rinsing with ethanol and water, the cantilever was immersed in water solution of 1-ethyl-3-(3-dimethylaminopropyl) carbodiimide hydrochloride (0.1 mol/L) and *N*-hydroxysuccinimide (0.05 mol/L) for 30 min. The cantilever was washed with water and immediately immersed in phosphate-buffered saline (PBS) solution of BSA (1 mg/mL) for 1.5 h at 37 °C. The BSA-immobilized cantilever was kept in PBS at 4 °C until use. The immobilization of proteins on the cantilever was confirmed using quartz crystal microbalance with dissipation (QCM-D) and XPS measurements by using a QCM gold sensor and gold-evaporated silicon wafer instead of the cantilever, respectively.

The adhesion force between BSA immobilized on the cantilever and BrC10DMCS-immobilized and polymer brush layers in PBS solution was evaluated from the approaching and retracting trace of force-versus-distance (f–d) curve at room temperature. The shift value of deflection in the retract trace of the f–d curves from the bottom of the retrace line corresponds to the adhesion force. In each measurement, more than 100 of the approaching/retracting f–d curves were collected, and the average value was defined as the adhesion force between BSA and substrates.

All measurements were repeated at least three times.

3. Results and discussion

3.1. Surface structure of polymer-grafted substrates

In this study, three kinds of polymer brush layers, PMPC, POEGMA, and PHEMA, were prepared on the BrC10DMCS-immobilized substrate using SI-ATRP with a free initiator. The semilogarithmic plot of monomer concentrations versus polymerization time, and the plot of molecular weight of the free polymers versus monomer conversion, remained linear during graft polymerization of the respective monomers from the BrC10DMCS-immobilized substrate, indicating the successful polymerization in the ATRP process [14]. At the end of the 24-h polymerization, the polydispersity of the respective free polymers was quite low (<1.3). Husseman et al. [24] and Yamamoto et al. [25] reported similarities in the properties of grafted polymers and polymers that formed in solution. Taking the reported results into account, the polymer brush layers prepared in this study would grow uniformly on the silicon wafer.

The surface elements of the polymer-grafted substrates were analyzed using the XPS spectra. The peaks of the carbon atom region (C_{1s}) at 285.0, 286.5, and 289.0 eV in all substrates corresponded to the neutral carbon, ether bond, and ester bond in the methacrylate group, respectively [14]. We detected the peaks of the phosphorus atom region (P_{2p}) at 133.0 eV, which corresponded to the phosphate group, and of the nitrogen atom region (N_{1s}) at 403.0 eV, which corresponded to the protonated ammonium group [14,26]. These peaks were specific to the phosphorylcholine group of the MPC unit. Thus, XPS analysis confirmed the identities of the monomer elements of each polymer chain on the surface of the silicon wafers.

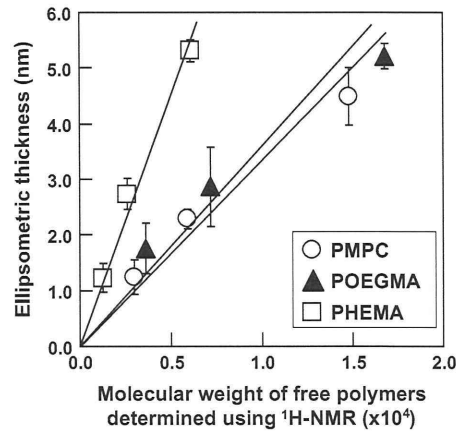

Fig. 2. Relationship between the absolute molecular weight of the polymer chains and the ellipsometric thickness of the grafted poly(2-methacryloyloxyethyl phosphorylcholine) (PMPC) layer (open circles), grafted poly(oligo(ethylene glycol) monomethacrylate) (POEGMA) layer (closed triangles), and grafted poly(2-hydroxyethyl methacrylate) (PHEMA) layer (open squares), under dry conditions.

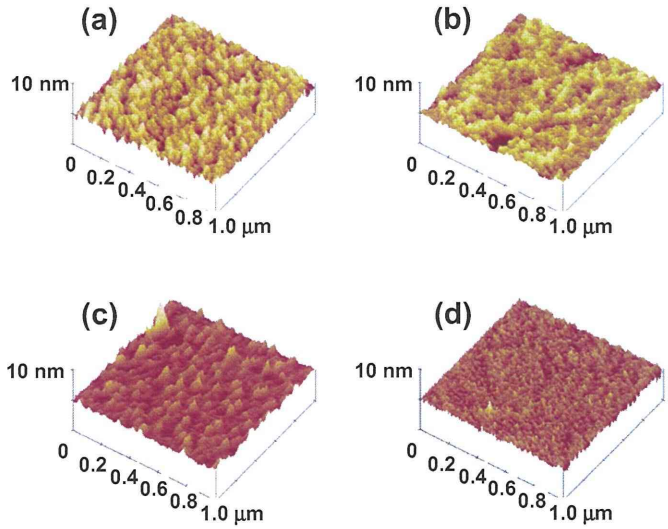

Fig. 3. Height images of (a) PMPC50 brush layer, (b) POEGMA50 brush layer, (c) PHEMA50 brush layer, and (d) BrC10DMCS-immobilized substrate, obtained by atomic force microscopy (AFM) under aqueous conditions.

The ellipsometric thickness values obtained for the grafted polymer layers under dry conditions were plotted against the absolute molecular weights of the polymer chains (Fig. 2). Thus, we demonstrated that the thickness of the grafted polymer layers could be linearly controlled in the range of 1–6 nm by controlling the molecular weight of the grafted polymer chains. We estimated the graft density of each polymer chain on the BrC10DMCS-immobilized substrates by using the slope of the linear graph to determine the relationship between thickness and molecular weight (Fig. 2). The graft densities of the polymer chains in the PMPC, POEGMA, and PHEMA brush layers were 0.26, 0.27, and 0.59 chains/nm^2, respectively. The graft densities of all polymer chains were greater than 0.10 chains/nm^2, which indicates the formation of dense polymer brush layers [27].

The surface topology of the polymer brush layers was examined using an AFM under aqueous conditions (Fig. 3). The surface of the BrC10DMCS-immobilized substrate was nearly flat, with an RMS value of exactly 0.40 nm (Fig. 3d). The surface roughness of each polymer brush layer increased compared with that of the BrC10DMCS-immobilized substrate (maximum RMS value: 0.8 nm) (Fig. 3a–c). These values were comparable to the previously reported RMS values in dry conditions [26], thereby indicating that the polymer brush layers prepared by the SI-ATRP method were considerably homogeneous and hardly changed in response to environmental conditions.

We measured the static water contact angles under dry conditions and static air bubble contact angles in aqueous conditions at the polymer brush layers, and plotted them against the ellipsometric thickness of the grafted polymer layers (Fig. 4). The static water contact angle in dry conditions for the silicon wafer was <10°, whereas that for the BrC10DMCS-immobilized silicon wafer was >80° (Fig. 4A). The static water contact angles for the polymer brush layers were lower than that of the BrC10TCS-immobilized substrate, even for thin grafted polymer layers. In all polymer brush layers, the static water contact angle under dry conditions decreased with increase in the thickness of the grafted polymer layers. The static water contact angles under dry conditions for PMPC brush layers decreased rapidly at a polymer chain thickness

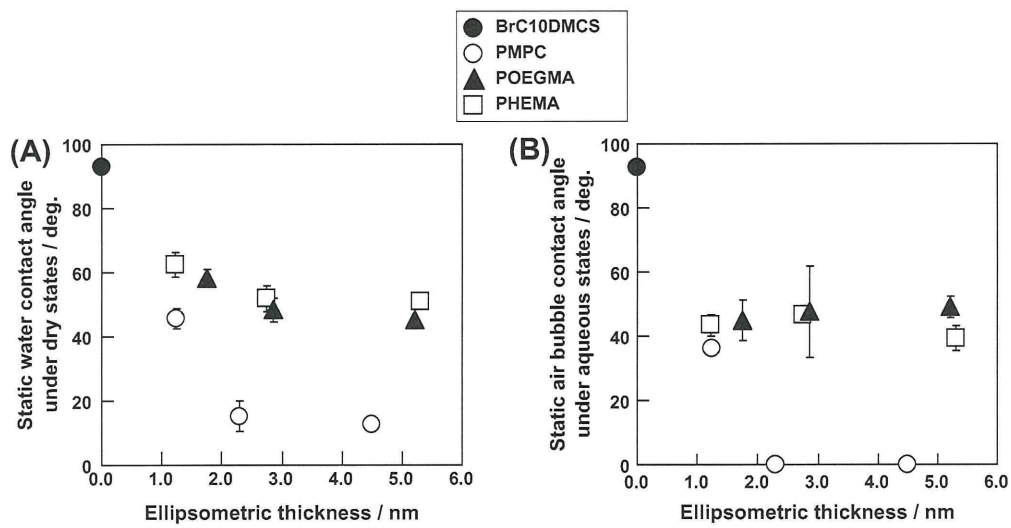

Fig. 4. (A) Static water contact angles under dry conditions and (B) static air bubble contact angles under wet conditions of the BrC10DMCS-immobilized substrate (closed circle), PMPC brush layers (open circles), POEGMA brush layers (closed triangles), and PHEMA brush layers (open squares).

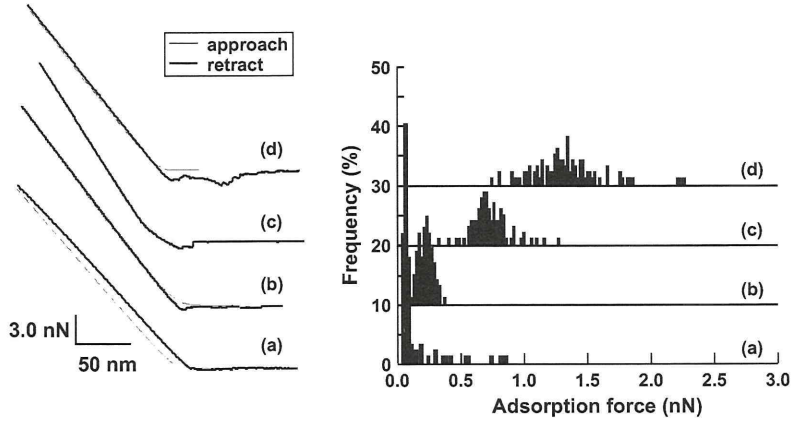

Fig. 5. (Left) Representative force-versus-distance curves between bovine serum albumin (BSA)-immobilized cantilever and polymer brush layers, and (Right) histograms of adhesion force of BSA against the polymer brush layers: (a) PMPC10 brush layer, (b) POEGMA10 brush layer, (c) PHEMA10 brush layer, and (d) BrC10DMCS-immobilized substrate.

of 2.0 nm, and then changed more slowly at approximately 10° at higher thickness values. On the other hand, the static water contact angles under dry conditions for the POEGMA and PHEMA brush layers were approximately 50° in the thick grafted polymer layers. Additionally, the static air bubble contact angles in aqueous conditions in all polymer brush layers did not change compared with the static water contact angles in dry conditions, indicating that the surface energy of the polymer brush layers remained constant in both conditions. Particularly, the high resistance to air bubbles in aqueous conditions of the thicker PMPC brush layers demonstrates that higher thickness confers high surface energy in aqueous media.

3.2. Adhesion force of proteins against polymer-grafted substrates

The extremely high repellency against protein adsorption of the hydrophilic polymer brush layers makes it difficult to discuss the slight differences in protein adsorption mass between the chemical structures of the polymer brush layers. Indeed, the amount of proteins adsorbed on PMPC, POEGMA, and PHEMA brush layers quantified by QCM measurement or radiolabeled proteins seems to be near the measurement limitation [9,10]. In this regard, the adhesion force of proteins against the surface of materials would be an important parameter that determines the protein adsorption behaviors at the interface.

Before the measurement of adhesion force of proteins against the polymer brush layers, the successful immobilization of proteins on the cantilever was confirmed by using QCM-D and XPS measurements (data not shown). From the QCM-D profiles, there was little difference in the BSA-immobilization process between with or without activation of COOH-SAM by WSC/NHS solution. The result indicated that the characteristics of the immobilized BSA on the cantilever surface are similar to that of the adsorbed BSA on the COOH-SAM [28,29].

Fig. 5 shows the representative *f–d* curves for the approach and retraction of a BSA-immobilized cantilever from the polymer brush layers or BrC10DMCS-immobilized substrates. In the case of the hydrophobic BrC10DMCS-immobilized substrate, the adhesion force of BSA was detected far from the outermost surface (up to 100 nm), and the top of the adhesion force was large (ca. 1.5 nN). On the other hand, the adhesion force of BSA was quite small and detected in a short range from the surface of the polymer brush layers. The high and long-ranged adhesion force against the BrC10DMCS-immobilized substrate indicates that the adsorbed BSA on the BrC10DMCS-immobilized substrate could hardly detach from the surface. Fig. 5 also shows the representative histograms of adhesion force of BSA against the thin polymer brush layers and BrC10DMCS-immobilized substrates from more than 100 *f–d* curves. The distribution of the adhesion force of BSA against the substrates could be fitted to Gaussian models and varied between different kinds of substrates. That is, the adhesion force against the BrC10DMCS-immobilized substrate had a broad distribution and large average value compared with that against the polymer brush layers with relatively thin layer thickness. Among the polymer brush layers, the adhesion force of BSA against the PHEMA10 brush layer was higher than against the other thin polymer brush layers. Fig. 6 shows the dependence on layer thickness of the polymer brush layers with different monomer units on the adhesion force of BSA against them. The adhesion force of BSA against the polymer brush layers decreased with the increase in layer thickness. This result was similar to previously reported results that the amount of the adsorbed proteins on the polymer brush surface depended on the thickness of the layer [10]. Furthermore, there was little difference in the adhesion force of BSA against the thick polymer brush layers among the chemical structures of monomer unit compared with the thin polymer brush layers. These results demonstrate the particularity of the polymer brush layer compared with the conventional materials that the thickness of the polymer brush layer has a relatively larger influence on the adhesion force of proteins than the chemical structure of the polymer brush layers. The proteins immobilized on the cantilever would maintain

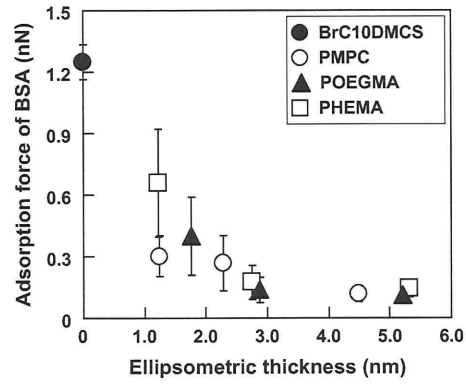

Fig. 6. Relationship between adhesion force of BSA and ellipsometric thickness at the PMPC brush layers (open circles), POEGMA brush layers (close triangles), PHEMA brush layers (open squares), and BrC10DMCS-immobilized substrate (closed circle).

their activity during the short measurement time of the *f–d* curves, while the conformation of proteins adsorbed on a surface would gradually change during the long measurement time for the protein adsorption mass. To better clarify the adhesion force of proteins against the polymer brush layers, the species and conformation of the proteins immobilized on the cantilever should be controlled. We are currently investigating the adhesion force of other or denatured proteins against polymer brush layers composed of hydrophilic monomer moieties, and hope to report these findings in the near future.

4. Conclusion

We synthesized three kinds of polymer brush layers, namely, PMPC, POEGMA, and PHEMA, on silicon wafers by using the SI-ATRP method. The graft density of polymer chains on the surface was high enough to form dense polymer brush layers. The surface roughness of the polymer brush layers under aqueous conditions analyzed using the AFM height images was quite low regardless of the structure of the monomer units. The wettability by water and resistance to air bubbles increased with the increase in thickness of the grafted polymer layers, and particularly, the PMPC brush layer had rather high surface energy. The adhesion force of BSA on the polymer brush layers decreased with increasing thickness of the grafted polymer layer, and finally reached an almost similar value among the different chemical structures. From these results, we conclude that the thickness of the polymer brush layer has a relatively larger influence on the adhesion force of proteins than the chemical structure of the polymer brush layers. We believe that the direct measurement of adhesion force of proteins against the nanostructure-controlled polymer brush layers would be a promising method to help elucidate the relationship among surface structure, surface properties, and protein adsorption behavior on the surface of biomaterials.

Acknowledgements

The authors thank Prof. Madoka Takai and Dr. Ryosuke Matsuno, The University of Tokyo, for helpful discussion on this research.

References

[1] H. Chen, L. Yuan, W. Song, Z. Wu, D. Li, Prog. Polym. Sci. 33 (2008) 1059–1087.
[2] E. Ostuni, R.G. Chapman, R.E. Holmlin, S. Takayama, G.M. Whitesides, A. Survey, Langmuir 17 (2001) 5605–5620.
[3] W. Norde, D. Gage, Langmuir 20 (2004) 4162–4167.
[4] G.L. Kenausis, J. Voros, D.L. Elbert, N. Huang, R. Hofer, L. Ruiz-Taylor, M. Textor, J.A. Hubbell, N.D. Spencer, J. Phys. Chem. B 104 (2000) 3298–3309.
[5] K. Ishihara, T. Ueda, N. Nakabayashi, Polym. J. 22 (1990) 355–360.
[6] K. Ishihara, H. Nomura, T. Mihara, K. Kurita, Y. Iwasaki, N. Nakabayashi, J. Biomed. Mater. Res. 39 (1998) 323–330.
[7] Y. Inoue, J. Watanabe, K. Ishihara, J. Colloid Interface Sci. 274 (2004) 465–471.
[8] Y. Goto, R. Matsuno, T. Konno, M. Takai, K. Ishihara, Biomacromolecules 9 (2008) 828–833.
[9] C. Yoshikawa, A. Goto, Y. Tsujii, T. Fukuda, T. Kimura, K. Yamamoto, A. Kishida, Macromolecules 39 (2006) 2284–2290.
[10] W. Feng, S. Zhu, K. Ishihara, J.L. Brash, Biointerphases 1 (2006) 50–60.
[11] Z. Wu, H. Chen, X. Liu, Y. Zhang, D. Li, H. Huang, Langmuir 25 (2009) 2900–2906.
[12] C.R. Emmenegger, E. Brynda, T. Riedel, Z. Sedlakova, M. Houska, A.B. Alles, Langmuir 25 (2009) 6328–6333.
[13] R. Iwata, P. Suk-In, V.P. Hoven, A. Takahara, K. Akiyoshi, Y. Iwasaki, Biomacromolecules 5 (2004) 2308–2314.
[14] Y. Inoue, K. Ishihara, Reduction of protein adsorption on well-characterized polymer brush layers with varying chemical structures, Colloids Surf. B: Biointerfaces 81 (2010) 350–357.
[15] Z. Zhang, M. Zhang, S. Chen, T.A. Horbett, B.D. Ratner, S. Jiang, Biomaterials 29 (2008) 4285–4291.
[16] W. Yang, S. Chen, G. Cheng, H. Vaisocherová, H. Xue, W. Li, J. Zhang, S. Jiang, Langmuir 24 (2008) 9211–9214.
[17] W. Yang, H. Xue, W. Li, J. Zhang, S. Jiang, Langmuir 25 (2009) 11911–11916.
[18] Z. Zhang, H. Vaisocherová, G. Cheng, W. Yang, H. Xue, S. Jiang, Biomacromolecules 9 (2008) 2686–2692.
[19] A. Idiris, S. Kidoaki, K. Usui, T. Maki, H. Suzuki, M. Ito, M. Aoki, Y. Hayashizaki, T. Matsuda, Biomacromolecules 6 (2005) 2776–2784.
[20] N.W. Moore, D.J. Mulder, T.L. Kuhl, Langmuir 24 (2008) 1212–1218.
[21] S. Kidoaki, T. Matsuda, Langmuir 15 (1999) 7639–7646.
[22] S. Kidoaki, Y. Nakayama, T. Matsuda, Langmuir 17 (2001) 1080–1087.
[23] A. Ramakrishnan, R. Dhamodharan, J. Ruhe, Macromol. Rapid Commun. 23 (2002) 612–616.
[24] M. Husseman, E.E. Malmstrom, M. McNamara, M. Mate, D. Mecerreyes, D.G. Benoit, J.L. Hedrick, P. Mansky, E. Huang, T.P. Russell, C.J. Hawker, Macromolecules 32 (1999) 1424–1431.
[25] K. Yamamoto, Y. Miwa, H. Tanaka, M. Sakaguchi, S. Shimada, J. Polym. Sci. A: Polym. Chem. 40 (2002) 3350–3359.
[26] W. Feng, J. Brash, S. Zhu, J. Polym. Sci. Part A: Polym. Chem 42 (2004) 2931–2942.
[27] Y. Tsujii, K. Ohno, S. Yamamoto, A. Goto, T. Fukuda, Adv. Polym. Sci. 197 (2006) 1–45.
[28] C.D. Tidwell, S.I. Ertel, B.D. Ratner, B.J. Tarasevich, S. Atre, D.L. Allara, Langmuir 13 (1997) 3404–3413.
[29] B. Sivaraman, K.P. Fears, R.A. Latour, Langmuir 25 (2009) 3050–3056.

Nano Today (2011) 6, 61—74

available at www.sciencedirect.com

ScienceDirect

journal homepage: www.elsevier.com/locate/nanotoday

REVIEW

Integrated functional nanocolloids covered with artificial cell membranes for biomedical applications

Ryosuke Matsuno[a,c,d], **Kazuhiko Ishihara**[a,b,c,d,*]

[a] *Department of Materials Engineering, The University of Tokyo, 7-3-1 Hongo, Bunkyo-ku, Tokyo 113-8586, Japan*
[b] *Department of Bioengineering, School of Engineering, The University of Tokyo, 7-3-1 Hongo, Bunkyo-ku, Tokyo 113-8586, Japan*
[c] *Center for NanoBio Integration, The University of Tokyo, 7-3-1 Hongo, Bunkyo-ku, Tokyo 113-8586, Japan*
[d] *Core Research for Evolutional Science and Technology (CREST), Japan Science and Technology Agency, 5 Sanban-cho, Chiyoda-ku, Tokyo 102-0075, Japan*

Received 8 November 2010; received in revised form 14 December 2010; accepted 23 December 2010
Available online 17 January 2011

KEYWORDS
Nanocolloids;
Artificial cell membrane;
Surface modification;
2-Methacryloyloxyethyl phosphorylcholine (MPC) polymer;
Protein adsorption;
Cell adhesion

Summary The functionality of nanocolloids used in biomedical applications are subject to strong interference arising from significant interactions with biological components such as proteins and cells. Among the known examples of surface treatment of nanocolloids, the construction of an artificial cell membrane structure based on phospholipid polymers has proven effective in preventing the occurrence of biological reactions at the surface. Furthermore, certain bioactive molecules can be immobilized on the surface of the phospholipid polymer platform to generate bioaffinity for other biomolecules. This review describes preparation and characterization of integrated functional nanocolloids covered by artificial cell membrane structures and their performance in biomedical applications.

Introduction

Nanocolloids may be defined as nanometer-scale particles dispersed in a medium [1]. They are mainly composed of metals and metal oxides, polymers, semiconductors, and carbon nanotubes, and display exceptional physical and chemical characteristics relative to bulk materials. Nanocolloids can be dispersed into solutions to form suspensions since the interaction of the colloid surface with the solvent is strong enough to overcome density differences. The efficiency of catalysts that employ nanocolloids tends to be high due to the increased surface-to-volume ratios. At the nanometer-scale, size-dependent properties are often observed. For example, quantum confinement in semiconductor particles, surface plasmon resonance in certain metal particles and superparamagnetism in magnetic materials. Moreover, unique structures with various functions can be fabricated by assembly of nanocolloids [1,2]. The nanometer-scale sizes of these structures make them suitable for analysis of microscopic regions, such as targeted intracellular regions. Such nanocolloids are widely used in applications such as development of biomolecular-supported materials, specific stains, and thermally, magnetically, and optically responsive materials for

* Corresponding author at: Department of Materials Engineering, The University of Tokyo, 7-3-1 Hongo, Bunkyo-ku, Tokyo 113-8586, Japan. Tel.: +81 3 5841 7124; fax: +81 3 5841 8647.
E-mail address: ishihara@mpc.t.u-tokyo.ac.jp (K. Ishihara).

1748-0132/$ — see front matter © 2010 Elsevier Ltd. All rights reserved.
doi:10.1016/j.nantod.2010.12.009

analyses of microscopic regions. In addition, nanocolloids are actively used in pharmaceutical and biomedical applications such as carriers for drugs and biomolecules and as imaging reagents.

However, when the nanocolloids are applied to biological systems, they encounter problems due to their specific structures. Since nanocolloids possess high energy surfaces, uncontrolled aggregation of colloid particles due to attractive van der Waals forces or electrostatic interactions gives rise to microstructural inhomogeneities in the medium. Protein becomes randomly adsorbed to the nanocolloid surface and reduces the function of the nanocolloids according to the size effect. The nanocolloids become adsorbed onto the cell membrane and enter the cell by endocytosis in the cell culture medium. The nanocolloids occasionally induce unexpected cellular responses. Regardless of the application of nanocolloids under biological conditions, the functionalities of nanocolloids may be disrupted by these biological responses, which are induced by nonspecific protein adsorption. To avoid this problem, the surfaces of nanocolloids are engineered to be biocompatible and bioinert [3–7].

There are many methodologies, which may be used to modify the surface of nanocolloids to obtain bioinert surfaces. Examples include the coupling of protein layers or self-assembling peptides to the surface, or coupling of water-soluble polymers to the surface. A rational strategy involves the use of bio-derived molecules. An adsorbed layer of bioinert protein, such as bovine serum albumin (BSA) or casein provides protein adsorption resistance [8]. These proteins are amphiphilic and have been used in the enzyme-linked immunosorbent assay (ELISA) as a blocking agent. Dextran, a natural polysaccharide, is also used as a surface modification to prevent bio-fouling [9]. Water-soluble synthetic polymers, such as poly(ethylene oxide) and polyacrylamide derivatives can be grafted or coated onto nanocolloids [10,11]. The water-soluble polymer chains expand into the aqueous medium and generate a highly mobile hydrated layer that surrounds the nanocolloids. Thus, the steric hindrance due to polymer chains prevents aggregation of the nanocolloids.

Other possibilities for generating surface modifications have been researched using phospholipid derivatives. Phosphatidylcholines are natural phospholipids that form self-assembly nanocolloids as a result of molecular interactions, which generate liposomes and lipid microspheres [12]. These phospholipid nanocolloids are used as pharmaceutical devices for carrying bioactive reagents in the bloodstream. Phosphatidylcholines have good biocompatibility, but their stability is not sufficient to enable long-term circulation in the bloodstream. However, the phospholipid assembly is one of the best candidate platforms for providing biocompatible surfaces. Moreover, when proteins and polysaccharides are immobilized on the platform, they adopt essentially the same structures that they have when they are attached to the cell membrane. Examples of monomers bearing phospholipid polar groups, notably the phosphorylcholine (PC) group, have reported [13–19]. These monomers can be polymerized and copolymerized with other vinyl compounds with various functional groups. Thus, the phospholipid polymers obtained show an interesting property in an aqueous medium.

Among these phospholipid polymers, 2-methacryloyloxyethyl phosphorylcholine (MPC) polymers are the most successful biomaterials for improving the biocompatibility of the surfaces of medical devices. The MPC polymers have PC groups in their side chains and have variable chemical structures as a result of the copolymerization process (Fig. 1) [19]. Over the past decade it has been established that the molecular weight, chain length, polydispersivity, conformation, and composition of the polymers can be controlled using living radical polymerization technique such as atom transfer radical polymerization (ATRP) [20], reversible addition-fragmentation transfer (RAFT) polymerization [21] and photoinduced iniferter polymerization [22]. These polymerization methods have been applied for obtaining the MPC polymers [23–27]. The MPC polymers have hydrophilicity and are electrically neutral due to their zwitterionic structures. They have low-friction and fluidity in aqueous media and have stable conformations in high salt solution and over a wide pH range. They are also biologically inert and have resistance to protein adsorption and cell adhesion. Furthermore, they do not cause tissue immunoreactions [28–34]. Thus, the modification of nanocolloids with the MPC polymers provides a bioinert platform similar to a cell membrane. The surface functions multiple and integrated as an artificial cell membrane when specific proteins and polysaccharides are coupled.

In this review, we summarize applications of nanocolloids modified by the MPC polymers for control of surface properties. There are four primary groups of applications: (i) design of nanocolloids covered with PC groups, (ii) the use of amphiphilic phospholipid polymers as nanocolloids, (iii) covering of polymeric nanoparticles with phospholipid polymers and immobilized biomolecules, and (iv) functionalization of quantum dots (QDs) with phospholipid polymer systems for cellular imaging.

Design of nanocolloids covered with PC groups

Surface modification of nanocolloids with chemically bonded or physically adsorbed PC groups is attracting increased attention. This interest is driven by fundamental studies of interfacial phenomena and also by the prospect of improving surface wettability, lubricity, and dispersion. Nanocolloid materials covered with PC groups are employed in MPC polymer grafting as well as encapsulation with phospholipids for biomedical applications. Table 1 provides a summary of surface modifications of nanocolloids with PC groups. Fig. 2 shows concept for surface modification of nanocolloids with phospholipid molecules and phospholipid polymers. Simple encapsulation of nanocolloids with phospholipid molecules and their assembly is well-known method. Using the phospholipid polymers, a solvent evaporation process for physical coating of the nanoparticles and a surface initiated-grafting from the surface of the nanocolloids have been reported. These nanocolloids covered by the PC groups have been applied in the biomedical fields. The covering of the PC groups enables the colloids to maintain the function of the colloid core within a biological environment, and enhances the dispersibility and stability of the nanocolloids in

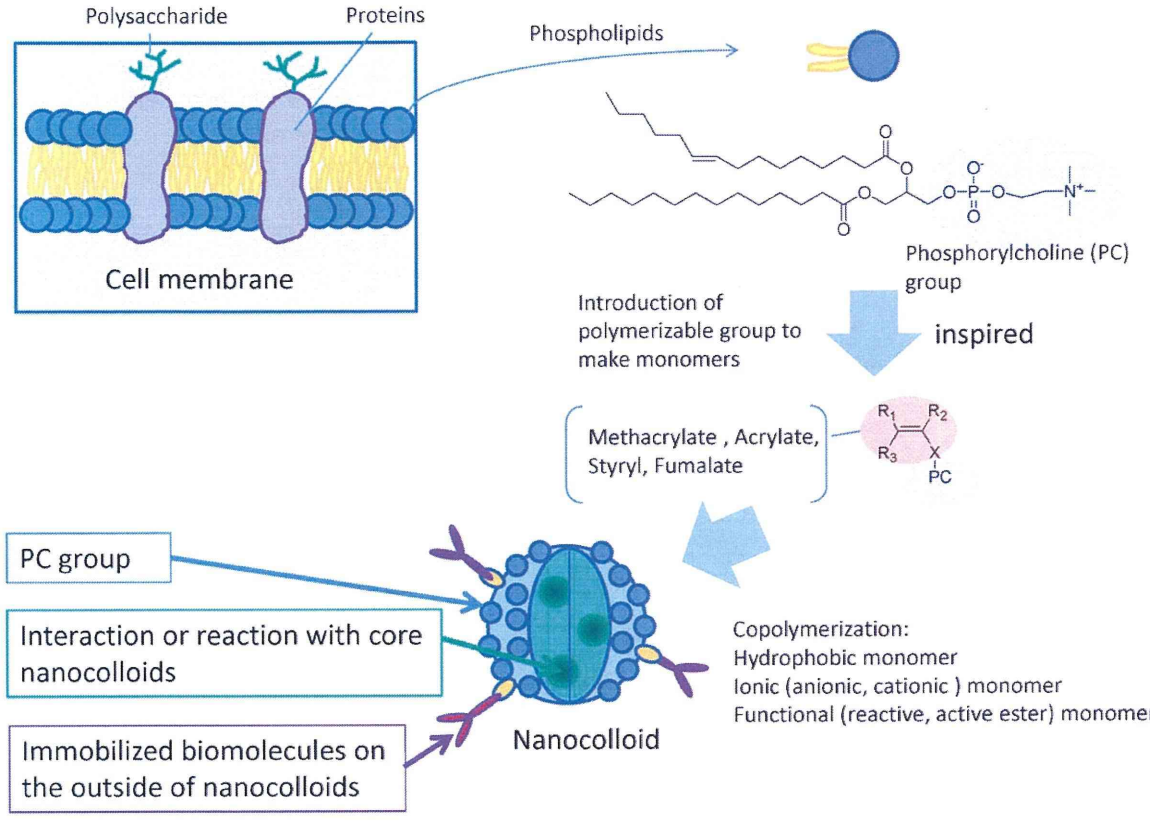

Figure 1 Functionalization of nanocolloids with phospholipid derivatives inspired from cell membrane.

Table 1 Surface modification of nanocolloid with PC group.

Core	Type of PC group	Function and biomedical potential	Ref.
SiO_2	Poly(MPC)	Nonthrombogenic materials	[35]
SiO_2	Poly(MPC)	Column Packing	[36]
SiO_2	Poly(MPC)	Analytical system	[37]
SiO_2	Trimethoxysilane derivative with PC group	Column Packing	[38]
SiO_2	DOPC	Biolabeling and Cellular Imaging	[39]
SiO_2, SnO_2	Poly(MPC) grafting	Stabilizer	[40]
SiO_2	Poly(MPC) grafting	Stabilizer	[41]
Au	Poly(MPC-*block*-DMA)	Detection system	[42]
Au	11-Mercaptoundecyl phosphorylcholine	Stabilizer	[43]
Au rod	11-Mercaptoundecyl phosphorylcholine	Cellular uptake and photothermal ablation	[44]
Ag	11-Mercaptoundecyl phosphorylcholine	Stabilizer	[45]
Ag	DSPC	Biosensing and Cell imaging tool	[46]
Fe_3O_4	Poly(MPC)	Magnetic separation	[47]
Fe_3O_4	Poly(MPC-*block*-DEA)	Imaging agent	[48]
Quantum dots	DPPC	Cell imaging tool	[49]
Carbon nanotube	Poly(MPC)	Analytical system	[50]
Carbon nanotube	POPC, BODIPY-PC	Biosensing	[51]
Polystyrene	DPPC	Lipid model	[52,53]
Polysaccharides	DPPC	Drug delivery	[54]

DOPC: 1,2-dioleoyl-sn-glycero-3-phosphocholine, DMA: 2-(*N*,*N*-dimethylamino)ethyl methacrylate, DSPC: bis(11,11′-dithiolundecyl) bis(1,1′-phosphorylcholine), DEA: 2-(*N*,*N*-diethylamino)ethyl methacrylate, DPPC: 1,2-dipalmitoyl-sn-glycero-3-phosphocholine, POPC: 1-palmitoyl-2-oleoyl-sn-glycero-3-phosphocholine, BODIPY-PC: 2-(4,4-difluoro-5-methyl-4-bora-3a,4a-diazas-indacene-3-dodecanoyl)-1-hexadecanoyl-sn-glycero-3-phosphocholine.

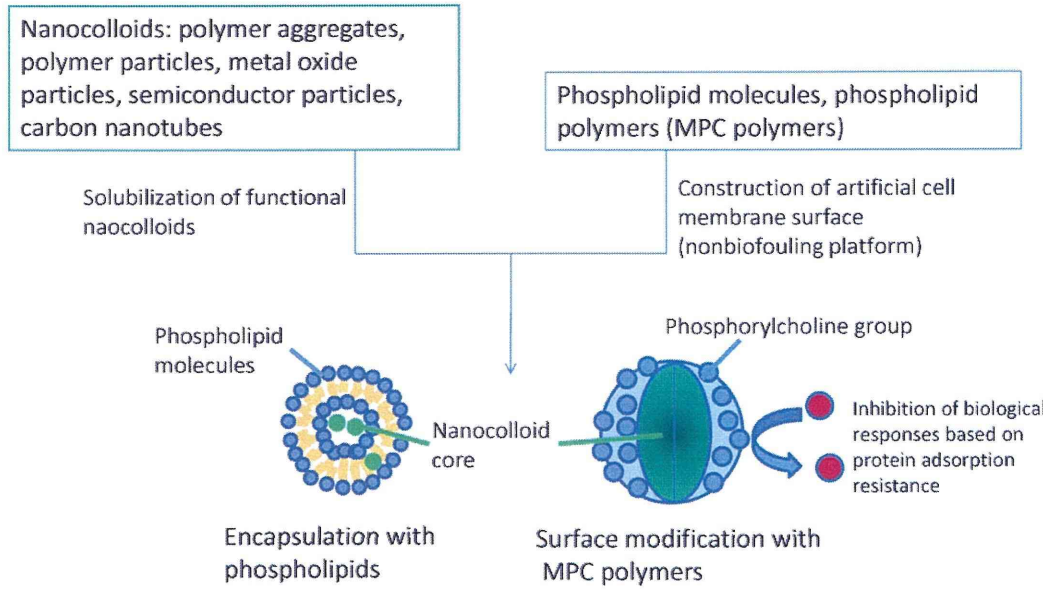

Figure 2 Hybridization of specific properties on nanocolloids by surface modification.

aqueous solution due to the prevention of adsorption of biomolecules.

Nanocolloids formed from inorganic compounds, semiconductor particles, or carbon nanotube cores have a wide range of functions and biomedical applications, which include uses as nonthrombogenic materials [35], column packing [36,38], analytical systems [37,50], cellular imaging [39,44,46,48,49], stabilizers [40,41,43,45], detection systems [42], magnetic separation systems [47], and biosensors [46,51]. Systems including nanocolloids with polymeric cores covered by PC groups have been also investigated as a lipid models [52,53] and drug delivery systems [54]. Surface modification by PC groups has been proven to be effective for biomedical applications.

Amphiphilic phospholipid polymers as nanocolloids

Although MPC polymer grafting is an effective method for providing a stable core, the method does not apply to unstable cores such as drugs, genes, and radical-sensitive materials. A simple strategy for modification of the unstable nanocolloid core involves the use of amphiphilic MPC polymer to form nanoparticles. This is induced by the presence of the MPC polymers themselves in aqueous solution. The MPC polymers may also be coated on core particles. Since amphiphilic MPC polymers with hydrophobic units form aggregations of micelles in aqueous medium via the driving force of hydrophobic interactions [55–59], the copolymers are available for solubilization of hydrophobic drugs or embedding of nanoparticles such as magnetic particles, semiconductors, and hydrophobic polymers. The amphiphilic MPC polymer with hydrophobic units and immobilization units enables integrated organization of nanobiodevices due to the dual-function provided by the core and surface. The amphiphilic MPC polymer with cationic units may be used to carry DNA vectors when DNA is condensed within the nanocolloids.

Drug delivery systems are used widely to treat diseases, especially cancerous tumors. The systems require many functions including biocompatibility, blood compatibility, hydrophilicity, and the capability to stabilize the loaded drug or DNA. Polymeric micelles consisting of amphiphilic polymers have gained increasing interest as drug carrier systems [60–62]. A representative polymer micelle formed with poly(ethylene oxide) has been used as a non-virus carrier because it is easy to control the copolymer composition, length, and shape [63]. MPC polymers are used in basic research and as drug carriers and as a shielding material for DNA vectors.

Tables 2 and 3 summarize the types of loaded drug or DNA, the MPC polymers, and immobilized biomolecules on the nanoparticles surface. Fig. 3 shows representative chemical structure of the MPC polymers. PMB, PMBN, and poly(MPC-*block*-cationic monomer) series copolymers have been mainly used as described below. Many drugs have low solubility in aqueous media. To solubilize hydrophobic drugs into aqueous media, amphiphilic MPC polymers have been investigated as drug carriers. As shown in Fig. 3, a representative copolymer is poly(MPC-co-*n*-butyl methacrylate (BMA)) (PMB) [64]. Among the PMB series with an MPC unit mole fraction of 30 mol%, the solubility of PMB against water can be controlled by the molecular weight. The water-soluble PMB30W polymer [65] (wherein ''30'' represents the unit mol% of MPC unit in PMB and ''W'' indicates solubility in water), with a molecular weight below 5×10^4 was found to be effective as a drug carrier. Surface tension measurements indicate that the surface tension of the PMB30W decreases from 10^{-2} mg/mL and becomes constant above 10^{-1} mg/mL [65]. Thus, PMB30W forms a polymeric micelle and a hydrophobic domain as a result of the formation of hydrophobic interactions of BMA in an aqueous medium. Recently, it is confirmed that the PMB can perme-

Table 2 Types of MPC polymers, loaded drug and immobilized biomolecules on the nanoparticles surface.

Polymer	Loaded drugs	Immobilized biomolecules	Diameter (nm)	Ref.
PMB	PTX	–	50	[67–69]
PLCG/PMB	SRL	–	<20	[72]
PMBN	PTX	HBs antigen	<50	[74]
PMBN	PTX	EGF	–	[75]
PMBN	PTX, FK506, CyA	IL-2	–	[76]
PMBH	Doxorubicin, PTX	Hydrazide (component of MPC polymer)	200	[77]
Poly(MPC-*block*-DPA)	Orange OT dye (not drug)	–	<30 (pH response)	[78]
Poly(FA-MPC-*block*-DPA)	Tamoxifen, PTX	Folic acid (end cap of poly(MPC) copolymer)	60–70 (pH response)	[81,82]
CMPC	ADR	–	<200	[83,84]
PIBr-Ch-g-PMPC (MPC was grafted from side chain)	PTX	–	7.5	[58]

PMB: poly(MPC-co-*n*-buthyl methacrylate(BMA)), PLCG: poly(L-lactide-co-caprolactone-co-glycolide), PMBN: poly(MPC-co-BMA-co-*p*-nitrophenylcarbonyloxyethyl methacrylate(MEONP)), PMBH: poly(MPC-co-BMA-co-methacryloyl hydrazide), FA: folic acid, DPA: *N,N*-diisopropylaminoethyl methacrylate, CMPC: cholessterol-end-capped poly(MPC), PIBr-Ch: poly(2-isopropyl-2-oxo-1, 3,2-dioxaphospholane-co-2-(2-oxo-1, 3, 2-dioxaphosphoroyloxyethyl-2-bromoisobutyrate-co-2-choresteryl-2-oxo-1, 3, 2-dioxaphospholane), PTX: paclitaxel, SRL: Sirolimus, CyA: cyclosporin A, ADR: adriamycin, HBs: hepatitis B surface, EGF: epidermal growth factor, IL: Interleukin.

Table 3 Types of MPC polymers, loaded DNA and immobilized biomolecules on the nanoparticles surface.

Polymer	Loaded DNA	Immobilized biomolecules	Diameter (nm)	Ref.
PMDN	sFlt-1 or GFP Plasmid DNA	HBs antigen	184 ± 54	[85]
Poly(MPC-*block*-DMA)	gWiz luc plasmid DNA	–	54.8 ± 12.9, 51.8 ± 12.2 (outer diameter of toroid, composition dependence	[86,87]
Poly(MPC-*block*-DEA)	Luciferase plasmid DNA, ODN	–	16.5×50.0 (cylinder fitting, charge ration of 1:1)	[88]
Poly(FA-MPC-*block*-DEA)	GFP Plasmid DNA	Folic acid (end cap of MPC polymer)	<200	[89]
Poly(DMAPAA-co-MPC-co-SA)	Plasmid DNA	–	280 ± 28, 290 ± 34 (before complex, composition dependence)	[90]
Poly(MPC-co-DAMA) (not target of the research)	Plasmid pCMVLacZ	–	230 ± 30 (N/P > 5)	[91]

PMDN: poly(MPC-co-*N,N*-dimethylaminoethyl methacrylate (DMA)-co-MEONP),DEA: *N,N*-diethylaminoethyl methacrylate, DMAPAA: N-[3-(dimethylamino)propyl] acrylamide, SA: stearyl acrylate, DAMA: 2-methyl-acrylic acid 2-[(2-(dimethylamino)-ethyl-methyl-amino]-ethyl ester, ODN: oligodeoxynucleotide, HBs: hepatitis B surface.

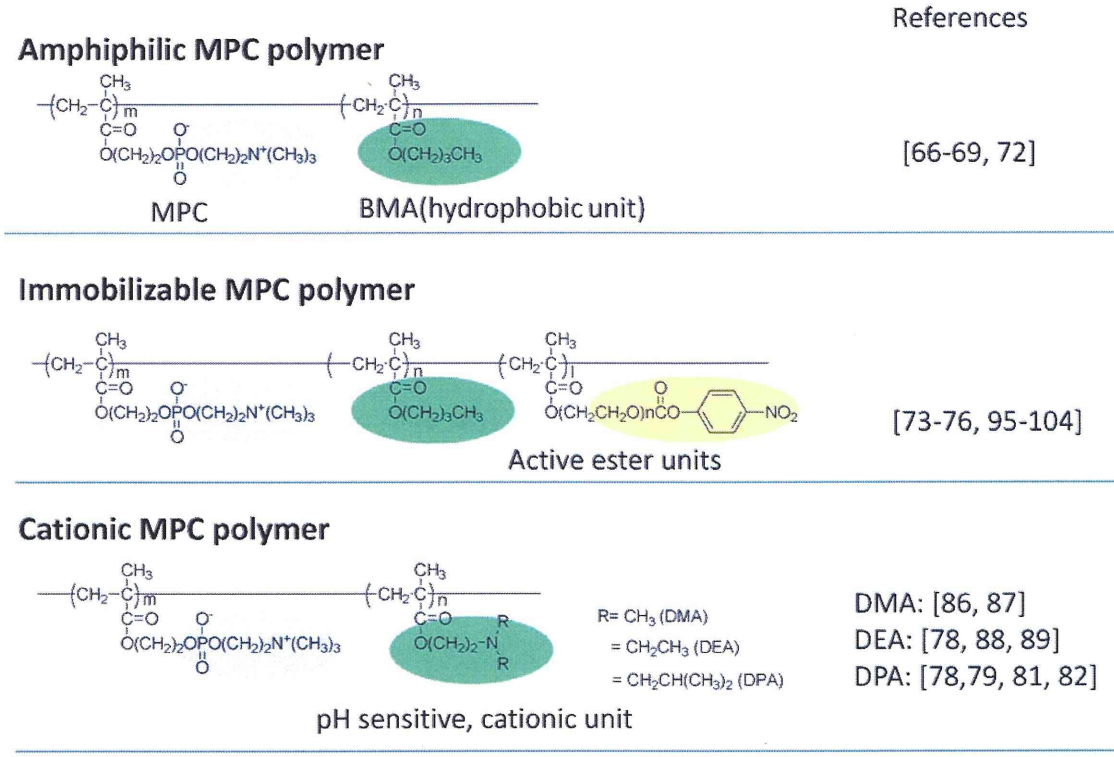

Figure 3 Chemical structure of representative phospholipid polymers, MPC polymers.

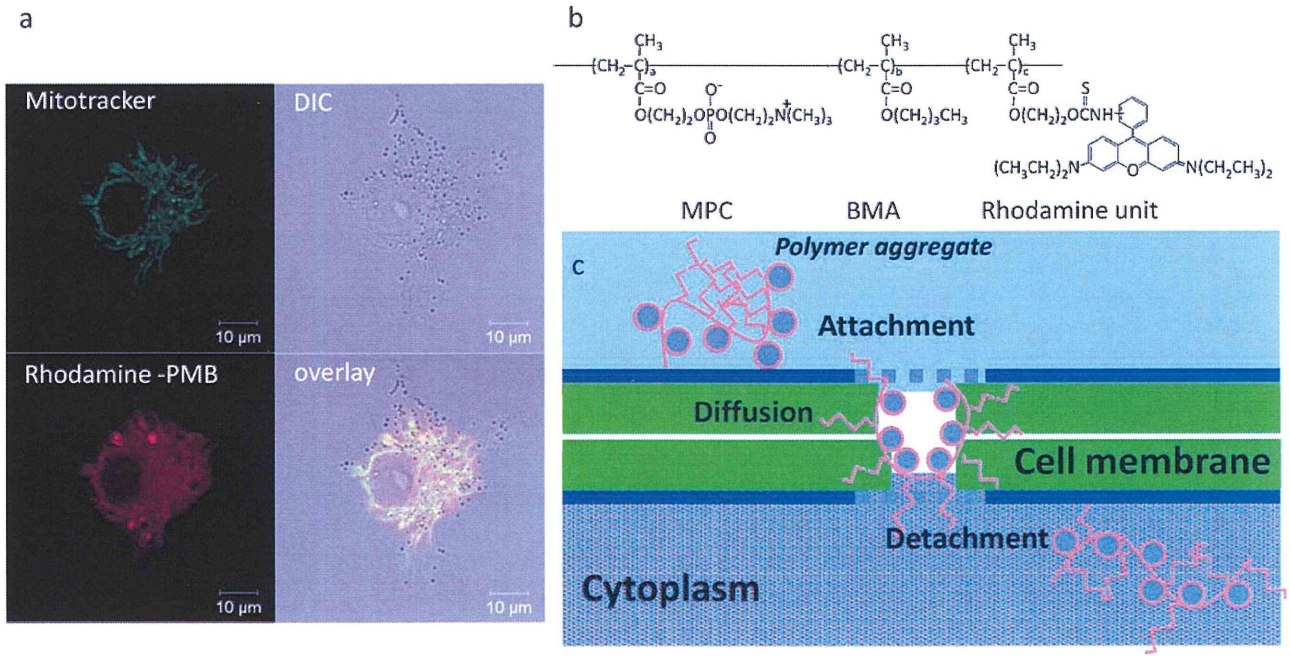

Figure 4 Direct penetration of PMB aggregates into cells by molecular diffusion mechanism [66]. (a) Confocal microscopic image after penetration of the rodamine-PMB, (b) chemical structure of rodamine-PMB, and (c) schematic representation of the diffusion mechanism through the cell membrane.

ate through the cell membrane by simple diffusion process, that is, energy-consuming endocytosis was not significantly [66]. When the PMB labeled with a specific fluorescence dye by copolymerization was introduced in cell culture medium, the inside of the cells stained within 1 min by the PMB diffusion. As the fluorescence dye, Rhodamine 6G has site-specificity to mitochondria in the cell, the Rhodamine-PMB concentrated at there (Fig. 4). This is due to flexible character of the polymer aggregate, the structure of the polymer aggregate may be changed during passing through the cell membrane.

Water-soluble and amphiphilic poly(MPC-co-BMA-co-*p*-nitrophenyloxycarbonyl poly(ethylene glycol) (MEONP)) (PMBN) were synthesized by radical polymerization [73]. An outer MEONP unit in an aqueous medium is capable of immobilizing proteins through the formation of a linkage between an active ester of MEONP and protein amino groups under mild conditions.

MPC polymers, which are responsive to pH, such as poly(MPC-*block*-2-(*N*,*N*-diethylaminoethyl methacrylate (DEA)) and poly(MPC-*block*-2-(*N*,*N*-diisopropylaminoethyl methacrylate (DPA)) were synthesized for drug delivery [78]. Poly(MPC-*block*-DPA) formed well-defined micelles at physiological pH to a greater extent than poly(MPC-*block*-DEA). Lowering of the pH of the solution was found to trigger the release of organic dye, Orange OT, due to the pKa of this component.

Polymer aggregate containing bioactive reagents

Paclitaxel (PTX), a well-known cancer drug, has poor solubility in aqueous media (<0.3 μg/mL). Konno et al. reported that the solubility of PTX could be enhanced using PMB30W (PMB30W/PTX) [67,68]. The concentration of PTX in PMB30W/PTX reached 5.0 mg/mL. The solution was transparent, and PTX did not precipitate even when the solution was stored at room temperature for 1 month. In a preliminary study, after an intravenous injection of mice with 200 mg/kg of the PMB30W aqueous solution, the mice remained calm and no weight loss was observed [67]. Soma et al. also evaluated the effect of intraperitoneal injection of PMB30W/PTX for treatment of gastric cancer. PMB30W/PTX was found to significantly reduce the numbers of metastatic nodules and to significantly reduce tumor volume relative to conventional dosages of PTX dissolved in Cremophor EL (Cremophor/PTX) [68].

Sirolimus (SRL) is a potent immunosuppressant, which inhibits the mammalian target of rapamycin, a central regulator of protein synthesis and cell growth [70]. However, SRL is an unstable agent. When degradation occurs, SRL produces an open-chain isomer, 34-hydroxy SRL, which retains less than 10% of the antiproliferative activity of the parent SRL [71]. Kim et al. reported the preparation of biodegradable polymer films for releasing nanovehicles containing SRL by combining PMB30W, poly(L-lactide-co-caprolactone-co-glycolide) (PLCG), and SRL [72]. PLCG/PMB30W/SRL films were found to reduce the production of 34-hydroxy SRL relative to PLCG/SRL films. The shielding effect provided by PMB30W nanovehicles suppresses the hydration of SRL.

Miyata et al. solubilized PTX into the hydrophobic domain of the PMBN to form a hybridized drug (PMBN/PTX) and then conjugated it with the preS1 domain of hepatitis B surface antigen for targeting IL-6 and/or immunoglobulin A binding protein [74]. Conjugation of preS1 to PMBN (preS1-PMBN) was found to strongly enhance the synergistic inhibitory effect of PTX on HepG2 cells. Shimada et al. reported the use of epidermal growth factor (EGF) conjugated to PMBN particles with PTX (EGF-PMBN/PTX) and its growth inhibitory and antitumor effects on cancer cells overexpressing EGF receptors [75]. The cytotoxicity and antitumor effects of EGF-PMBN/PTX were significantly greater than those of PMBN/PTX for EGFR-overexpressing cells, but not for an EGFR-deficient line. These results suggest that EGF-PMBN-PTX represents a more potent targeted therapy for tumors over-expressing of EGFR. Chiba et al. the showed that the proliferation of cell lines with high-affinity IL-2 receptors derived from T cell malignancies were suppressed by IL-2-conjugated (IL2-PMBN) with incorporation of PTX and cyclosporin A at lower concentrations than used conventionally [76]. IL2-PMBN-PTX was also found to inhibit the proliferation of responder cells in a human mixed lymphocyte culture at lower concentrations than the unconjugated drug.

Iwasaki et al. synthesized a water-soluble MPC polymer with hydrazide groups (PMBH) [77]. Unnatural carbohydrates with ketone groups on the cell surface of human cervical cells were obtained by treatment with levulinoyl mannosamine (ManLev) as shown in Fig. 5. The nanoparticles covered with PMB could not adhere on the cell, however, Those covered with PMBH indicated strong binding affinity to the cells. The PMBH nanoparticles immobilized with the anticancer drugs doxorubicin or PTX come into contact with either ManLev-treated or untreated cells. As a result, the anticancer drugs were selectively delivered to the ManLev-treated cell. Ligand-immobilized MPC polymers can thus be used as active targeting carriers.

A folic acid (FA)-functionalized poly(MPC-*block*-DPA) (FA-MPC-DPA) was synthesized [79]. It is well known that many malignant tissues such as ovarian, nasopharyngeal, cervical, and chorionic carcinomas consistently express high levels of folate receptors, which are accessible via the bloodstream [80]. FA has the potential to function as a tumor-targeting ligand for folate receptor. The FA-MPC-DPA micelles may be used to encapsulate PTX and tamoxifen, which are insoluble in water [81]. The loading capacity can be controlled by adjusting the composition of the block. Drug uptake studies on a colon carcinoma cell line have confirmed that FA-MPC-DPA loading of PTX and tamoxifen (approximately 100%) results in highly efficient drug uptake relative to poly(MPC-*block*-DPA). Approximately 100% of PTX and tamoxifen are loaded using FA-MPC-DPA vs 25% of tamoxifen and 40% of PTX for poly(MPC-*block*-DPA) [82]. Cholesterol-end-capped MPC polymer and poly(MPC)-grafted poly(dioxaphospholane) have also been synthesized as drug carriers [83,64,58].

Colloidal polymer complexes with DNA

Chiba et al. reported the use of cationic poly(MPC-co-*N*,*N*-dimethylaminoethyl methacrylate (DMAEMA)-co-MEONP) (PMDN) conjugated to hepatitis B surface (HBs) antigen for

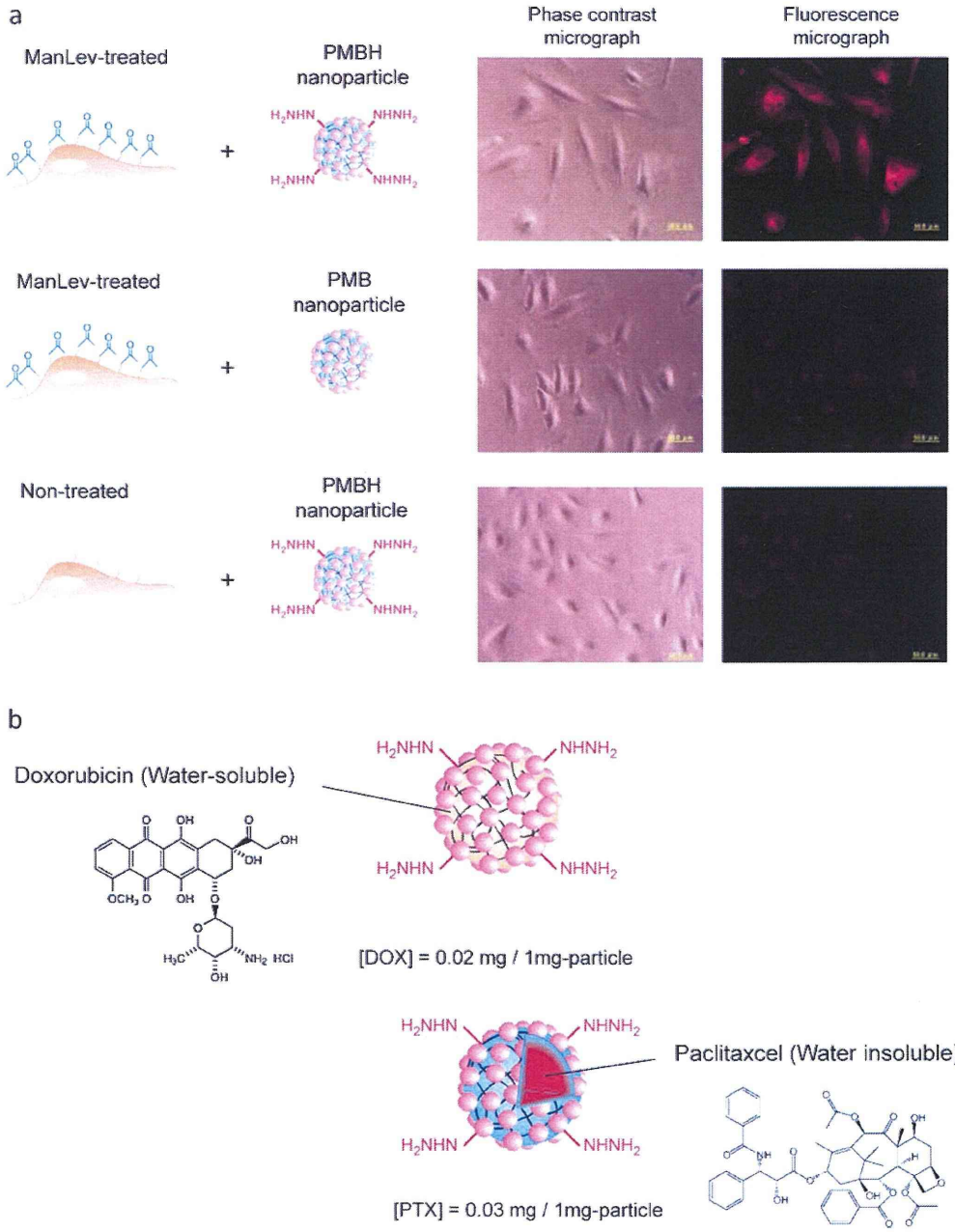

Figure 5 Cell-specific function of polymer nanoparticles covered with the hydrazide group modified MPC polymer (PMBH) [77]. (a) Specific interaction of PMBH with ketone group generated cells. (b) Schematic representation of anticancer drug-immobilized nanoparticles.

the specific transfer of genes into human hepatocytes [85]. The specific expression of sFlt-1 or GFP by PMDN conjugated to HBs containing plasmid (HBs-PMDN/plasmid), PMDN containing plasmid (PMDN/plasmid), plasmid only, and PBS were assessed in HepG2 and WiDr tumor cells *in vitro* and *in vivo*. The sFlt-1 and GFP expression was observed only in HepG2 cells transfected with sFlt-1 or HBS-PMDN/GFP. These results suggest that HBs-PMDN can function as a human hepatocyte-specific gene delivery vector without serious side effects.

Armes et al. reported a structural study of DNA condensation induced by poly(MPC-*block*-2-(*N*,*N*-dimethylaminoethyl methacrylate (DMA)) and poly(MPC-*block*-DEA) as a non-virus vector for gene delivery [86–88]. The cationic amino groups in the side chain interact with the anionic DNA molecules. The incorporation of an MPC moiety into the DEA polycation provides steric stabilization of the DNA polyplexes and reduces their non-specific cellular association *in vitro*. Poly(FA-MPC-*block*-DEA) was applied to a targeting gene delivery vector via folate receptor-mediated endocytosis

[89]. In MCF-7 and KB cells overexpressing folate receptors, the conjugated systems undergo folate-specific association and achieve significantly enhanced transfection efficiency, relative to the FA-nonconjugated control, with dramatically reduced nonspecific cellular association. On the other hand, the level of cellular association of FA-MPC-DEA was not statistically increased in A549 cells that have an undetectable level expression of folate receptors, relative to nonconjugated control. Targeting of ligand-immobilized or capped MPC polymer can also be used as an active targeting gene carrier. Additionally, MPC polymers with other cationic units such as N-(3-dimethylaminopropyl) acrylamide (DMAPAA) [90] or 2-[(2-(*N*,*N*-dimethylamino)ethylmethylamino)ethyl methacrylate (DAMA) [91], were synthesized for development of DNA vectors.

Multifunctional envelope-type nanocolloids

An integration system using a multifunctional envelope-type nano device (MEND) has significantly higher transfection activity relative to conventional gene delivery systems [92]. Harashima and coworkers have reported that modification of cholesteryl glutamic acid-alanine-leucine-alanine (GALA) peptide on the surface of MEND enhances fusion with the endosomal membrane and cytoplasmic release of encapsulated macromolecules [93]. It was recently reported that an additional coating of GALA-modified liposomes with PMB50 produces an enhancement in the transfection activity of encapsulating plasmid DNA, which is two orders of magnitude higher [94]. The MPC polymer coating decreases the zeta potential of GALA-modified liposomes. This suggests that the polymer coating assists in the functional display of negatively charged GALA on the cationic liposomes by providing shielding from mutual electrostatic interactions.

Polymeric nanoparticles covered with phospholipid polymers and immobilized biomolecules

To determine the amounts of specific molecules using biodevices within a biological environment, a molecular recognition reaction is required. The most useful method for this purpose is to employ biospecific molecular reactions such as antibody/antigen and enzyme/substrate reactions. The surfaces of the biodevices require effective immobilization of biomolecules, and maintenance of the activity of the biomolecules. Concurrently, non-specific binding of the target molecules should be inhibited. The excellent applicability of PMBN has been demonstrated in an ELISA system, a microchip immunoassay system and an immunosensor system as a blocking agent [95–97]. The coating of the MPC polymer for the large detection area of the sensor causes a decrease in noise level, which is attributed to non-specific binding and an increase in signal level. Thus, a high signal/noise (S/N) ratio is obtained. We provide a description of diagnosis probes, which employ polymer nanocolloids covered by the MPC polymer in an aqueous medium. The PMBN was easily deposited onto the surface of the polymer nanoparticles by the solvent evaporation method. Table 4 summarizes the immobilization of biomolecules on PMBN nanoparticles and applications in diagnosis.

Goto et al. evaluated the retention of the reactivity of antibody, which is immobilized on the nanoparticles and the selectivity with respect to the protein mixture [98]. The affinity binding of the BSA and anti-BSA antibody on the PMBN particles with poly(L-lactic acid) (PLA) core was examined as a model antigen/antibody interaction. The stability of antigen/antibody complexes with the antibody immobilized on PMBN/PLA-NP is the same as that in solution. This value is 100 times higher relative to the values measured for the antibody immobilized on conventional polystyrene nanoparticles. The selective binding of BSA as an antigen from a protein mixture, BSA, γ-globulins, and human plasma fibrinogen was found to be high relative to that observed with conventional antibody-immobilized polymer nanoparticles due to the effects of phosphorylcholine groups on the suppression of protein adsorption.

Watanabe et al. prepared polymer nanoparticles for sequential enzymatic reactions by combining PMBN with a polystyrene core with a diameter of ca. 360 nm [99]. For the sequential enzymatic reactions, acetylcholine esterase, choline oxidase, and horseradish peroxidase-labeled IgG were individually immobilized onto the nanoparticles. Acetylcholine chloride, choline chloride, and tetramethylbenzidine were added as substrates to the suspension of the nanoparticles. The acetylcholine chloride was converted to choline chloride. The choline chloride was oxidized by choline oxidase, and then hydrogen peroxide was formed as an enzymatic degradation product. The hydrogen peroxide was used for a subsequent enzymatic reaction involving oxidization of tetramethylbenzidine by the peroxidase. The rates of the sequential enzymatic reactions taking place on the nanoparticles via hydrogen peroxide were significantly higher than the corresponding reaction rates in the enzyme mixture. This indicates that the diffusion pathway of the enzymatic products, and the localization of the immobilized enzyme are important aspects of these reactions.

Bimolecular recognition for instantaneous determination using a fluorescence resonance energy transfer (FRET) system-installed PMBN particle was also investigated [101]. C-reactive protein (CRP) and osteopontin (OPN) were used as the target biomarkers for the instantaneous determination. The resulting fluorescence intensity correlated well with changes in the concentrations of the target molecules. The immunoassay protocol simply involves mixing of FRET-installed NPs and target molecules such as CRP and OPN antigens. Additionally, these immunoassays were found to be capable of detecting the existence of interfering molecules.

Konno et al. prepared two types of enzyme co-immobilized particles and applied them in the development of a microdialysis biosensor [100]. The PMBN was used as an emulsifier and a surface modifier to prepare the PLA nanoparticles with diameter of ca. 200 nm. Both acetylcholine esterase and choline oxidase were co-immobilized (dual-mode conjugation). The enzymatic reactions on the nanoparticles were followed using a microdialysis biosensor system with a microtype hydrogen peroxide electrode in the probe. The nanoparticles enabled detection of acetylcholine chloride as hydrogen peroxide, which is a product of the continuous enzymatic reactions occurring on the surface of the nanoparticles in the probe. It was concluded that

Table 4 Function of nanoparticles covered with PMBN for diagnosis probe.

Core	Immobilized biomolecules	Contents and applications	Diameter (nm)	Ref.
PLA	Anti-albumin antibody	High affinity separation system for proteins	<290	[98]
PSt	Acetylcholinesterase, choline oxidase, and horseradish peroxidase-labeled IgG	Sequential enzyme reaction	ca. 360	[99]
PLA	Acetylcholine esterase and choline oxidase	Microdialysis biosensor	ca. 200	[100]
PSt	Alexa Fluor 488-labeld anti-CRP-IgG, and Alexa Fluor 555-labelded anti-OPN-IgG	Biomolecular recognition system by FRET	190	[101]
PLA	Anti-CRP monoclonal antibody	CRP-detection system	205–654	[102]
PLA	Luciferase	Microdialysis biosensor	ca. 200	[103]
PLA	Anti-IgG antibody, alkaline phosphatase	Medical treatment agent	ca. 200	[104]

PLA: poly(L-lactic acid), PSt: polystyrene, CRP, C-reactive protein, OPN: osteopontin, IgG: immunoglobulin G, FRET: fluorescence resonance energy transfer.

the nanoparticles are a promising tool for development of a highly sensitive microdiagnostic system.

Ito et al. investigated dual mode reactions on PMBN particles [104]. Both an anti-mouse IgG antibody and an alkaline phosphatase enzyme were immobilized on the nanoparticles and the antigen/antibody reaction and enzymatic reaction, were both observed. When an antigen was added to the suspension of the nanoparticles, aggregation and precipitation of the nanoparticles occurred. The enzymatic reaction proceeded efficiently when the enzyme substrate was added to the suspension. The novel polymer nanoparticles could be used for nano-/micro-scaled diagnostic and medical treatment systems. In addition, a diagnosis probe using PMBN was applied to a C-creative protein-detection system [102], and a microdialysis biosensor [103].

Functionalization of quantum dots with phospholipid polymer

The development of bioimaging technologies for medicine, pharmacology, and biology is an important research area. Fluorescence imaging with an adaptable fluorescence probe is widely used in life sciences because of it is non-invasive. As described above poly(MPC) has excellent protein adsorption resistance and cell adhesion resistance. Consequently, a bioimaging probe with a stable and highly sensitive fluorescence probe covered by poly(MPC) is incapable of penetrating into cells by itself. To facilitate penetration, the probe has been integrated with cell-penetrating peptides and embedded with QDs. In the next section, we discuss bioimaging probes using poly(MPC).

Direct modification of QDs

QDs ranging in size between 2 and 6 nm have unique optical properties. Their emission spectra are material- and size-dependent, and their absorption spectrum is wide. They have high quantum yields, exhibit simultaneous multicolor emissions, and have excellent resistance to photo-bleaching. In biological applications, QDs have been widely used for *in vitro* applications such as cell labeling [105,106], tracking cell migration [107,108], and fluorescence resonance energy transfer [109,110] and for *in vivo* applications such as contrast agents of tumor-tissue sections [111], imaging of prostate cancer [112], and sentinel-lymph-node mapping in pigs [113]. Obviously, to obtain a stable and highly sensitive bioimaging fluorescence probe without cytotoxicity under cell culture medium, the surface of the QDs must be coated by biomolecules or water-soluble polymers because the QD surface is generally covered by hydrophobic ligands such as trioctylphosphine oxide (TOPO) [114].

Matsuno et al. reported a poly(MPC) grafted onto a QD (CdSe/ZnS) surface using a new strategy involving the use of a double functional RAFT agent to develop a biocompatible polymer modification method [115]. As the first function, the RAFT agent has surface activity that forms a micelle in aqueous solution and solubilizes the TOPO-coated QD into the solution. As the second function, the RAFT agent has chain transfer agent ability that synthesizes a poly(MPC)-grafted QD in an aqueous medium. The RAFT polymerization initiates at the surface of QDs treated with the RAFT agent. The MPC polymer chains formed are immobilized stably at the surface. The poly(MPC)-modified QD has good biocompatibility based on the poly(MPC) properties and was able to suppress uptake by HeLa cells despite the fact that the diameter of the poly(MPC)-modified QD was approximately 12 nm.

QDs embedded in polymeric nanoparticles covered with phospholipid polymer

Goto et al. prepared PMBN nanoparticles with embedded QDs with diameters of ca. 20 nm [116,117]. When the surface of the PMBN/PLA nanoparticles is reacted with glysine through active ester group in the MEONP unit, the polymer nanoparticles without cell-penetrating peptides showed resistance to cellular uptake from HeLa cells owing to the nature of the phosphorylcholine groups. On the other hand,

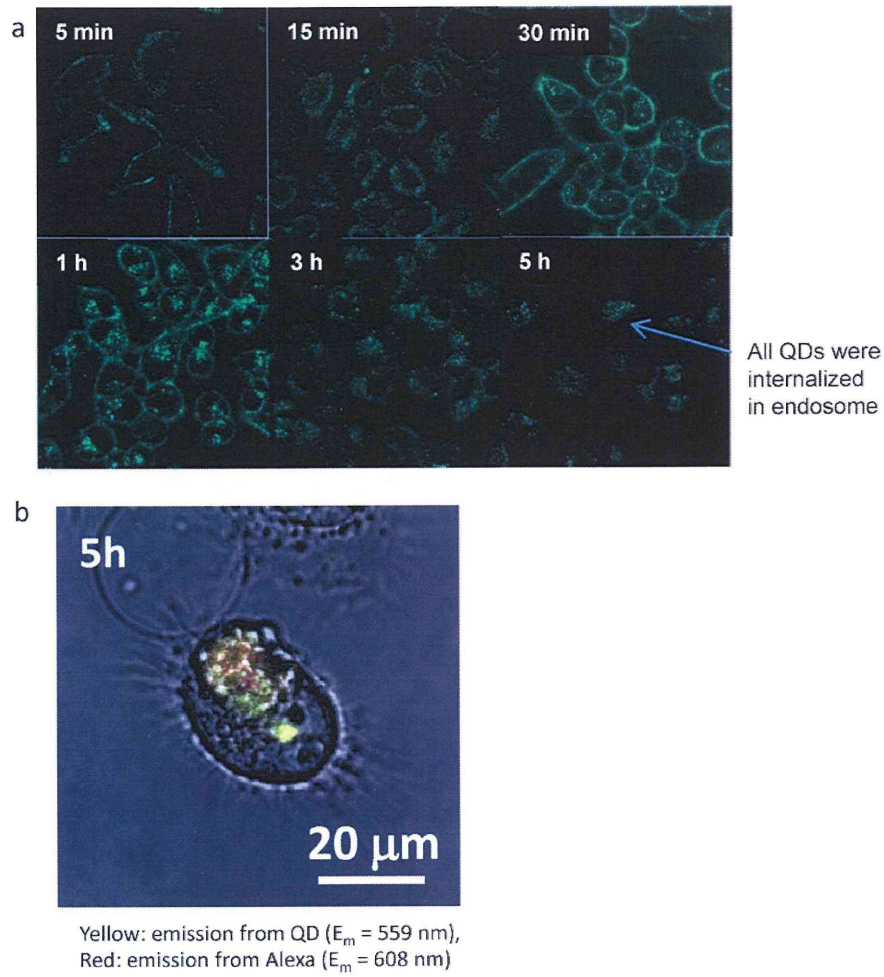

Figure 6 Cellular uptake of the MPC polymers-modified QDs as imaging probe. (a) Real-time confocal microscopic image of R8-PMBN/PLA nanoparticles embedding QDs in HeLa cells through endocytosis process [117]. (b) pH imaging by FRET between MPC polymer-immobilized QD and fluorescence dye probe in HeLa cells [118].

when arginine octapeptide (R8) was immobilized at the surface of the nanoparticles through an active ester in MEONP, the nanoparticles were able to penetrate the membrane of HeLa cells effectively without cytotoxicity through the process of endocytosis shown in Fig. 6(a). This indicates that the function of immobilized R8 was not affected by surrounding MPC polymers.

Recently, Masuda et al. prepared a fluorescence probe, which exhibits a combination of pH response and changes in fluorescence spectra for detection of cellular pH responses [100]. The nanoparticles were composed of a QD core and a block-type water-soluble poly(MPC) with a pH-responsive poly(DEA) segment as a shell. After Alexa 594 cadaverine dye was immobilized via MEONP located on the outer surface, the FRET efficiency between the QD core and Alexa was observed in aqueous media at pH 7.4 and pH 5.5. These pH values initiate the process of endocytosis as a result of the proton sponge effect. The fluorescence spectra undergo changes between pH 7.4 and pH 5.5 because the distance between QD and Alexa changes according to the pKa 7.1 of the poly(DEA) chain. Thus, when the distance between the QD core and Alexa is within several nm at pH 7.4, FRET arises from QD as a donor to Alexa as an acceptor. This produces an increase in fluorescence intensity of Alexa with a red color. When the distance is far at pH 5.5 due to protonation, independent fluorescence of QD and Alexa are observed. A color change of the poly(MPC) nanoparticles resulting from the arrest of endocytosis was observed after injection into HeLa cells, which were cultured for 5 h (Fig. 6(b)). Yellow and red colors indicate emissions from QD (E_m = 559 nm) and from Alexa (E_m = 608 nm), respectively. According to the process of endocytosis, the red color indicates arrest of endocytosis in the endosome at pH 5.5 to the cytosol at pH 7.4.

Future perspectives

Fortunately, when poly(MPC) is synthesized, there is no need to worry about reduction of the biocompatibility over a wide range of molecular weights because the biocompatibility of poly(MPC) is independent of molecular weight. Therefore, many kinds of MPC polymers have been designed and synthesized to have flexibility for use in several applications. As described in this paper, it has been demonstrated that

poly(MPC) provides the means to control nanodevices using nanocolloids. The representative PMB, PMBN, and poly(MPC-*block*-cationic unit) polymers are useful for applications including delivery of biomolecules, and development of diagnosis probes and bioimaging probes using nanocolloids. Poly(MPC) concentrated on nanodevices surface provides the high shielding effect required for protein adsorption without interruption to provide immobilized biomolecules on the surfaces. The arrangement is a key to achieving a biointerface. New investigations have indicated that effective integration with amphiphilic MPC polymers and other devices produced good results. In one example, the combination of GALA-modified MEND with PMB50 resulted in enhancement of the transfection activity of encapsulating plasmid DNA by two orders of magnitude. The integration is expected to identify new fields of research.

The structure of MPC is inspired from a part of the phospholipid structure. This structure feedback from biomolecules represents a rational strategy for obtaining new biocompatible material. However, with respect to biocompatibility, phospholipids are the only known useful compounds existing in nature. There is thus a need for development of new material to provide different feedback. Over past decade, research has been active on the hydration states of biomaterials. It has been revealed that possession of a common hydration state is important for biocompatible polymers as well as proteins. Thus, as a first step toward obtaining new materials, "mechanism feedback" from the hydration state is required. Presently, the hydration state cannot be assessed with respect to biocompatibility on the basis of chemical structure. Research on the biocompatibility of the hydration state will be required to obtain the next generation of "feedback materials."

Acknowledgments

We thank Prof. Madoka Takai, Prof. Tomohiro Konno, and Dr. Yuuki Inoue, of the University of Tokyo for their helpful discussions during the preparation of this manuscript.

References

[1] C.B. Murray, C.R. Kagan, M.G. Bawendi, Annu. Rev. Mater. Sci. 30 (2000) 545–610.
[2] A. Zabet-Khosousi, A.-A. Dhirani, Chem. Rev. 108 (2008) 4072–4124.
[3] P. Aggarwal, J.B. Hall, C.B. McLeland, M.A. Dobrovolskaia, S.E. McNeil, Adv. Drug Deliv. Rev. 61 (2009) 428–437.
[4] M.A. Phillips, M.L. Gram, N.A. Peppas, Nano Today 5 (2010) 143–159.
[5] T. Lammers, V. Subr, K. Ulbrich, W.E. Hennink, G. Storm, F. Kiessling, Nano Today 5 (2010) 197–212.
[6] N. Wiradharma, Y. Zhang, S. Venkataraman, J.L. Hedrick, Y.Y. Yang, Nano Today 4 (2009) 302–317.
[7] L. Zhang, T.J. Webster, Nano Today 4 (2009) 66–80.
[8] R.V. Vogt Jr., D.L. Phillips, L.O. Henderson, W. Whitfield, F.W. Spierto, J. Immunol. Meth. 101 (1987) 43–50.
[9] R. Huynh, F. Chaubet, J. Jozefonvicz, Carbohydrate Res. 332 (2001) 75–83.
[10] C. Barrera, A.P. Herrera, C. Rinaldi, J. Colloid Interface Sci. 329 (2009) 107–113.
[11] T.Y. Liu, S.H. Hu, D.M. Liu, S.Y. Chen, I.W. Chen, Nano Today 4 (2009) 52–65.
[12] N.T.K. Thanh, L.A.W. Green, Nano Today 5 (2010) 213–230.
[13] K. Sugiyama, K. Ohga, H. Aoki, N. Amaya, Macromol. Chem. Phys. 196 (1995) 1907–1916.
[14] T. Oishi, T. Fukuda, H. Uchiyama, F. Kondou, H. Ohe, H. Tsutsumi, Polymer 38 (1997) 3109–3115.
[15] A. Kros, M. Gerritsen, J. Murk, J.A. Jansen, N.A.J.M. Sommerdijk, R.J.M. Nolte, J. Polym. Sci. Polym. Chem. 39 (2001) 468–474.
[16] K. Miyazawa, F.M. Winnik, Macromolecules 35 (2002) 2440–2444.
[17] K. Kratz, K. Breitenkamp, R. Hule, D. Pochan, T. Emrick, Macromolecules 42 (2009) 3227–3229.
[18] P. Kujawa, G. Schmauch, T. Viitala, A. Badia, F.M. Winnik, Biomacromolecules 8 (2007) 3169–3176.
[19] K. Ishihara, T. Ueda, N. Nakabayashi, Polym. J. 22 (1990) 355–360.
[20] J.S. Wang, K. Matyjaszewski, J. Am. Chem. Soc. 117 (1995) 5614–5615.
[21] J. Chiefari, Y.K. Chong, F. Ercole, J. Krstina, T.P.T. Le, R.T.A. Mayadunne, G.F. Meijs, G. Moad, C.L. Moad, E. Rizzardo, S.H. Thang, Macromolecules 31 (1998) 5559–5562.
[22] T. Otsu, J. Polym, Sci. Part A; Polym. Chem. 38 (2000) 2121–2136.
[23] E.J. Lobb, I. Ma, N.C. Billingham, S.P. Armes, J. Am. Chem. Soc. 123 (2001) 7913–7914.
[24] I.Y. Ma, E.J. Lobb, N.C. Billingham, S.P. Armes, A.L. Lewis, A.W. Lloyd, J. Salvage, Macromolecules 35 (2002) 9306–9314.
[25] S.-I. Yusa, K. Fukuda, T. Yamamoto, K. Ishihara, Y. Morishima, Biomacromolecules 6 (2005) 663–670.
[26] Y. Inoue, J. Watanabe, M. Takai, S.-I. Yusa, K. Ishihara, J. Polym. Sci. Part A; Polym. Chem. 43 (2005) 6073–6083.
[27] D. Miyamoto, J. Watanabe, K. Ishihara, Biomaterials 25 (2004) 71–76.
[28] K. Ishihara, M. Takai, J. R. Soc. Interface 6 (2009) S279–S291.
[29] R. Matsuno, K. Ishihara, Macromol. Symp. 279 (2009) 125–131.
[30] M. Kobayashi, H. Yamaguchi, Y. Terayama, Z. Wang, K. Ishihara, M. Hino, A. Takahara, Macromol. Symp. 279 (2009) 79–87.
[31] J. Watanabe, K. Ishihara, Colloids Surf. B: Biointerfaces 65 (2008) 155–165.
[32] K. Ishihara, K. Nishizawa, Y. Goto, M. Takai, Adv. Sci. Technol. 57 (2008) 5–14.
[33] J. Watanabe, K. Ishihara, Kobunshi Ronbunshu 63 (2006) 548–559.
[34] T. Moro, Y. Takatori, K. Ishihara, T. Konno, Y. Takigawa, T. Matsushita, U.I. Chung, K. Nakamura, H. Kawaguchi, Nat. Mater. 3 (2004) 829–836.
[35] R. Yokoyama, S. Suzuki, K. Shirai, T. Yamauchi, N. Tsubokawa, M. Tsuchimochi, Eur. Polym. J. 42 (2006) 3221–3229.
[36] W. Jiang, G. Fischer, Y. Girmay, K. Irgum, J. Chromatogr. A 1127 (2006) 82–91.
[37] Y. Matsuda, M. Kobayashi, M. Annaka, K. Ishihara, A. Takahara, Langmuir 24 (2008) 8772–8778.
[38] Y. Watanabe, M. Abolhassani, Y. Tojo, Y. Suda, K. Miyazawa, Y. Igarashi, K. Sakuma, T. Ogawa, K. Muramoto, J. Chromatogr. A 1216 (2009) 8563–8566.
[39] M.D. Senarath-Yapa, S. Phimphivong, J.W. Coym, M.J. Wirth, C.A. Aspinwall, S.S. Saavedra, Langmuir 23 (2007) 12624–12633.
[40] X.Y. Chen, S.P. Armes, S.J. Greaves, J.F. Watts, Langmuir 20 (2004) 587–595.
[41] C.-D. Vo, A. Schmid, S.P. Armes, K. Sakai, S. Biggs, Langmuir 23 (2007) 408–413.
[42] J.J. Yuan, A. Schmid, S.P. Armes, Langmuir 22 (2006) 11022–11027.
[43] Q. Jin, J.-P. Xu, J. Ji, J.-C. Shen, Chem. Commun. (2008) 3058–3060.